NJC

New Journal of Chemistry

A journal for new directions in chemistry

Accepted Manuscript

This article can be cited before page numbers have been issued, to do this please use: S. A. E. Abdel-Latif, Y. Issa, A. L. Elansary and H. B. Hassib, *New J. Chem.*, 2020, DOI: 10.1039/D0NJ05397J.

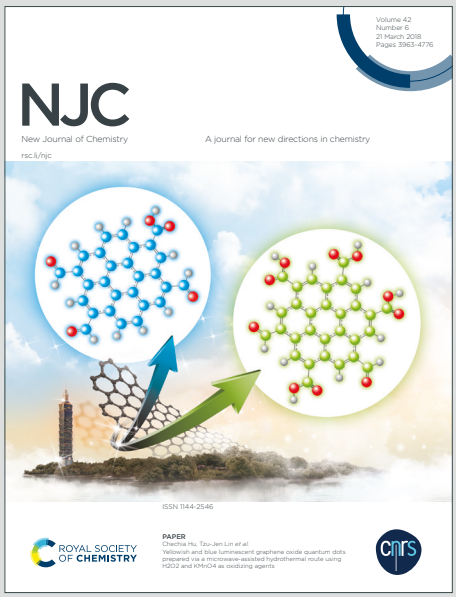

This is an Accepted Manuscript, which has been through the Royal Society of Chemistry peer review process and has been accepted for publication.

Accepted Manuscripts are published online shortly after acceptance, before technical editing, formatting and proof reading. Using this free service, authors can make their results available to the community, in citable form, before we publish the edited article. We will replace this Accepted Manuscript with the edited and formatted Advance Article as soon as it is available.

You can find more information about Accepted Manuscripts in the Information for Authors.

Please note that technical editing may introduce minor changes to the text and/or graphics, which may alter content. The journal's standard Terms & Conditions and the Ethical guidelines still apply. In no event shall the Royal Society of Chemistry be held responsible for any errors or omissions in this Accepted Manuscript or any consequences arising from the use of any information it contains.

Synthesis, spectroscopic characterization, DFT/TD-DFT/PCM calculations of molecular structure and NBO of novel charge-transfer complexes of pyrazine Schiff base derivatives with aromatic nitro compounds

Yousry M. Issa[a], Samir A. Abdel-Latif[b,] Aida L. El-Ansary[a] and Hekmat B. Hassib[a]*
[a]Chemistry Department, Faculty of Science, Cairo University, Giza, 12613, Egypt.
[b]Chemistry Department, Faculty of Science, Helwan University, Cairo, 11795, Egypt.

Novel Charge-transfer (CT) solid complexes of pyrazine Schiff bases, derived from 2-aminopyrazine and substituted benzaldehydes (N-benzylidenepyrazin-2-amine, (NBPA) and N-(4-dimethylamino)benzylidene)pyrazin-2-amine) (NDMABPA) with some aromatic nitro compounds have been synthesized and characterized experimentally using ultraviolet-visible (UV-Vis.) absorption, infrared spectra and proton nuclear magnetic resonance (^{1}HNMR) spectroscopy, the complexes were formed in a mole ratio of 1:1, with good indications for existing charge-transfer in its molecular structure. Theoretical studies were done on donors and acceptors elucidating their structures and the active sites where the charge-transfer occurs. The experimental work was done in ethanol. The solution characterizations included the determination of the molecular structure of the formed CT complexes where it verified 1:1 (donor:acceptor) in ethanol. Quantum mechanical calculations of geometries, energies were attained using the density functional theory with Becke's three parameter exchange functional method, the Lee-Yang-Parr correlation functional approach (B3LYP/DFT) combined with 6.31G(d,p) basis set has been consecutively out in solution using ethanol as solvent to compliment the measured results and to justify the CT within the donors and the acceptors. The optimized energy, complexation energy, geometrical parameters, Natural atomic charges as well as 3D-plots of the molecular electrostatic potential maps (MEP) were computed and elucidated; they resided with the experimental results where the complexes stability are attributed to the presence of charge-transfer. The electronic spectra

* Corresponding author. Chemistry Department, Faculty of Science, Helwan University, Cairo, Egypt
Email: SAMIR_ABDO@science.helwan.edu.eg (S. A. Abdel-Latif)

were computed and executed using time dependent-density functional theory (TD-DFT) via adding polarizable continuum solvation method PCM, PCM-TD-DFT. The allowed singlet transitions are positioned and their highest occupied molecular orbital (HOMO) and lowest unoccupied molecular orbital (LUMO) involvements are represented. The describes of the frontier HOMO and LUMO molecular orbitals, contributing in the first four singlet transitions were showed. For all the formed solid complexes, the main relations between the donors and the acceptor molecules take place through the π-π* interaction. Secondary n-π* transition was noticed in some complexes. The vibrational wavenumbers have also been performed using B3LYP/6-31G(d,p) and the results matches the experimental one. The small energy gap between HOMO and LUMO energies expressions that the CT occurs within the donors and the acceptors. Hyper conjugative interactions, molecular stability, bond strength and intramolecular CT have been investigated by applying natural bond orbital (NBO) analysis. Mean polarizability, total static dipole moment, anisotropy of polarizability and mean first-order hyperpolarizability have been also attained. The obtained values show that the CT complexes are accomplished candidate to non-linear optical (NLO) materials.

Keywords: Aminopyrazine, Schiff bases, Charge-transfer complexes, Spectroscopic studies, DFT/TD-DFT calculations, non-linear optical properties.

Introduction

Numerous investigations have been created concerning the charge-transfer complexes of aromatic nitro materials with several aromatic donor compounds.[1-5] Such studies were devoted to evaluating the ionization potential of donors, or electron empathies of acceptors as well as the consequence of π-π* bonding in complex construction. Limited studies are involved with CT complexes of Schiff bases.[6,7] Hindawey et al.[8] studied the solid complexes of p-nitrophenol, some dinitro and trinitrobenzenes with p-substituted benzylidenaniline. The formed complexes of some hydroxyl Schiff bases with poly nitrobenzenes were studied.[9] Complexes of the donor-acceptor type formed between aromatic amines and π-acceptors were the subject of widespread studies.[10-12] N-heterocyclic compounds were used as effective donors in the formulation of CT complexes with different p-benzoquinone products.[13,14] The proton transfer complex of 2-amino-4-hydroxy-6-methylpyrimidine with salicylic acid has

been separated and their crystal developed by slow evaporation technique.[15] A new CT complex incorporating hydrogen bonding between the e-donor 3-amino-1,5-dimethylpyrazole with the e-acceptor chloranilic acid has been created and characterized experimentally and theoretically.[16] A novel CT complex between the n- and π-donor of 5-amino-1,3-dimethylpyrazole with the π-acceptor chloranilic acid was produced and illustrated experimentally and theoretically. The experimental work was performed in solution and solid state.[17] Charge-transfer interactions between the electron donor gliclazide and the p-acceptors 2,3-dichloro-5,6-dicyano-1,4-benzoquinone and tetracyanoethylene were investigated in chloroform as solvent and in the solid state,[18] New CT complex formed between the n- and p-donor 1-Benzoylpiperazine with p- acceptor p-chloranil were carried out in polar solvent (acetonitrile) at several temperatures. The formed 1:1 chemical composition of the CT complex is verified.[19] The crystal and molecular structures of two novel separated CT complexes created from the reaction of tris(hydroxymethyl)aminomethane and 2,5-dichloro-3,6-dihydroxy-1,4-benzoquinone (chloranilic acid) in the mole ratios of 2:1 and 1:1, have been studied and characterized.[20] The chemistry of an organic CT complex between pyrazole donor and chloranilic acid acceptor has been studied in ethanol at room temperature. The created complex has been described by different techniques.[21] CT complexes of 4-(2-thiazolylazo) resorcinol with 3,5-DNSA, PA, and CLA were made and depicted spectroscopically and theoretically. Molecular structure of the formed complexes was established in methanol.[22] A molecule (2E)-3-(biphenyl-4-yl)-1-(4-bromophenyl) prop-2-en-1-one was separated, and the structure has been distinguished by using spectroscopic techniques. DFT method were used within B3LYP/6–311++G(d,p) basis set to optimize the molecular structure of the formed compound. Vibrational wavenumbers, geometrical parameters and electronic properties have also been achieved.[23] The CT complex of 1-benzoylpiperazine as a donor with the π-acceptor 2,3-dichloro-5,6-dicyano-p-benzoquinone has been examined spectrophotometrically in acetonitrile at various temperatures. The computational analysis of the CT complex using density functional theory adopts the experimental work. The charge transfer in the CT complex and its extreme stability are showed through both experimental and theoretical studies.[24]

The present article deals with the preparation of CT complexes of some pyrazine Schiff bases with di-and tri-nitrobenzene products and studied using IR, ^{1}H-NMR and UV visible spectroscopy to characterize the type of bonding between the donor and acceptor molecules in the formed CT complexes. Theoretical computations by means of

the density functional theory (DFT) at the basis set B3LYP/6-311 G(d,p) will be included to study the ground state properties as geometrical parameters, optimization structure, reactivity parameters and 3D-plots of the molecular electrostatic potential maps (MEP). The derivation of electronic spectra and the composition of the frontier molecular orbitals will be examined using TD-DFT through the polarizable continuum solvation model (PCM). The natural population analysis will be employed to compute the natural atomic charge of each site of the complexes and natural bond order analysis to study the inter- and intra-molecular CT in the constructed complexes. The reliability between measured and computed results is the significant purpose of this work.

Experimental

Materials and apparatus

All chemicals used in this study were pure grade BDH and Fluka chemicals. They include 2-aminopyrazine, benzaldehyde, p-N-dimethylbenzaldehyde, picric, 3,5-dinitrosalicylic, 3,5-dinitrobenzoic acids and Nujol. The organic solvents used were, dimethylsulfoxide (DMSO) and ethanol. The solvents were purified by recommended methods.[25]

Preparation of Schiff bases (Donors)

The aminopyrazine Schiff bases used in this investigation were synthesized by condensation of equivalent amounts of 2-aminopyrazine and the corresponding aldehydes; benzaldehyde or p-N-dimethylbenzaldehyde. 0.1 mole of 2-aminopyrazine was mixed thoroughly with 0.1 mole of aldehyde in 250 mL ground flask. About 100 mL of ethyl alcohol were added and the mixture was refluxed for four hours. The product separated after cooling, collected and recrystallized from hot ethanol till constant m.p.[26] The obtained Schiff bases have the resulting structural formulae (Scheme 1), their colors, melting points and elemental analysis are listed in Table 1:

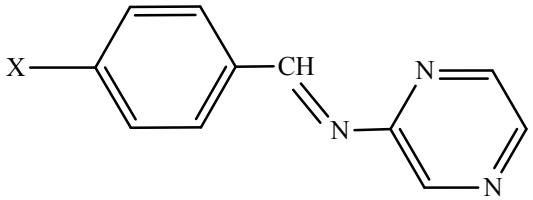

Where X = H, N-benzylidenepyrazin-2-amine, (NBPA)

= p-N$(CH_3)_2$, N-(4-dimethylamino)benzylidene)pyrazin-2-amine, (NDMABPA)

Scheme 1. Structure of the prepared donors

View Article Online
DOI: 10.1039/D0NJ05397J

Table 1 Color, melting points and elemental analyses of 2-aminopyrazine Schiff bases

X	Color	M. P. °C	C% Calc. (Found)	H% Calc. (Found)	N% Calc. (Found)
H	Light-brown	116	72.04 (71.83|)	4.91 (5.10)	22.92 (22.65)
p-$N(CH_3)_2$	Green-yellow	60	68.94 (69.70)	6.19 (6.60)	24.75 (24.35)

Preparation of charge-transfer complexes

The donors used in the preparation of the CT complexes were the prepared Schiff bases. The acceptors used are picric (PA), 3,5-dinitrosalicylic (3,5-DNSA) and 3,5-dinitrobenzoic (3,5-DNBA) acids. The 1:1 CT complexes were prepared by mixing a hot alcoholic saturated solution of the donor (0.01 mole dissolved in the least amount of hot ethanol) with an equimolecular amount of the acceptor as described previously.[27] The solid complexes were separated immediately (picric acid) or on standing (p-N-dimethylbenzalhedyde), they recrystallized from ethanol. The complexes obtained displayed various colors depending on the donor and acceptor used. The products then filtered off, dried and their melting points determined, Table 1.

Physical measurements

The IR spectra were attained by using a Shimadzu FT-IR spectrometer in the range 4000-400 cm^{-1} applying the KBr disc technique. The ^{1}H-NMR spectra of the Schiff bases and their CT complexes were recorded using Varian 300 MHz NMR spectrometer at room temperature using TMS (tetramethylsilan) as an internal standard and d_6 dimethylsulphoxide (DMSO) provided from Merck used as solvent. The electronic absorption spectra were examined within the visible and ultraviolet ranges (800-200 nm) using the same solvent as blank and determined using Perkin-Elmer lambda 4B UV-Vis spectrophotometer. $1x10^{-3}$ mol/L stock solutions of the donors and their CT complexes were prepared via dissolving the accurate weight in 25 mL of ethanol as solvent. The measured concentrations were prepared by diluting the exact volume in 10 mL of ethanol. Measurements covered the ranges from 210-400 nm and 230-700 nm for the Schiff bases and their CT complexes, respectively. Nujol Mull method was used in which sample is combined with Nujol in a mortar to make a mull which is then positioned in the spectrophotometer.

Computational Details

Owing to the absence of single crystal X-ray structure analysis and to obtain the molecular conformation of the donors and their CT complexes, energy minimization analyses were done by means of Gaussian-09W software package.[28] The ground state geometrical structures of the donors and their CT complexes were optimized by means of the density functional theory with Becke's three parameter exchange functional method,[29] the Lee-Yang-Parr correlation functional (B3LYP) and the split-valence double zeta basis set with two polarized basis functions (d and p), (DFT/B3LYP) at the 6-31G(d,p) with the B3LYP exchange correlation functional approach.[30] The basis set 6-31G(d,p) was applied for C, H, N and O atoms,[31-33] respectively. Through geometry optimizations, every bond length, bond angle and dihedral angle could relax free of constraints, the geometry of the considered systems was totally optimized in gas-phase. Several properties can be analysed using the DFT theory such as optimization energy, geometrical parameters, 3D-plots of the molecular electrostatic potential maps (MEP) and reactivity parameters. Gauss-View 5 software,[34] Avogadro and Chemcraft programs have been used to extract the calculated results, and visualize the optimized forms, the frontier molecular orbitals and 3D-plots of the molecular electrostatic potential (MEP) maps. The quantum chemical parameters of the donors and their CT complexes are gained from calculations as energies of the lowest unoccupied molecular orbital (E_{LUMO}), the highest occupied molecular orbital (E_{HOMO}), HOMO-LUMO energy gap, E_g, absolute electronegativities, χ, chemical potentials, π, absolute hardness, η, absolute softness, σ, global electrophilicity, ω, global softness, S, and additional electronic charge, ΔN_{max}. These parameters are computed using these equations;[35,36] $E_g = E_{LUMO} - E_{HOMO}$, $\chi = - E_{HOMO} + E_{LUMO}/2$, $\eta = E_{LUMO} - E_{HOMO}/2$, $\sigma = 1/\eta$, $\pi = -\chi$, $S = 1/2\eta$, $\omega = \pi^2/2\eta$ and $\Delta N_{max.} = -\pi/\eta$. The spin density difference map computations were also performed to explain their optical properties. Natural bond orbital (NBO) calculations were performed[37] with the NBO code contained in Gaussian 09 to understand different second order interaction between the filled orbital of one subsystem and vacant orbital of another subsystem which is the calculate of the molecular delocalization or hyperconjugation. The mean polarizability ($<\alpha>$), the anisotropy of the polarizability ($\Delta\alpha$), the mean first order hyperpolarizability ($<\beta>$) and the total static dipole-moment (μ) via the x, y, z components were analyzed.[38-40] TD-DFT computations were brought out at the same level of theory (B3LYP/6-31G(d,p)) to elucidate the origin of electronic spectra, using polarizable continuum solvation method PCM, PCM-TD-DFT. In PCM the solute part lying inside cavity, whereas the solvent part (ethanol) denoted as a

structureless matter. In PCM method, the solvent is also considered by its dielectric constant and other macroscopic parameters. The vibrational frequency calculations were achieved utilizing the same level of theory (B3LYP/6-31G(d,p)) to confirm that the found optimized geometries stand for local minima.

Results and Discussion

CT complexes are formed through primary interaction invoking the transfer of one electron from the highest occupied molecular orbital on the donor molecule to the lowest unoccupied molecular orbital on the acceptor molecule (π-π* HOMO → LUMO transition). In addition, secondary interactions are liable to occur depending on the nature of acceptor and donor molecules. These include n-π* interactions. HOMO → LUMO investigation was undertaken to elucidate the origin of both the intramolecular interaction of the free Schiff bases and the intermolecular CT interaction with electron acceptors. The IR bands of the CT complexes compared with those of the respective free donor[41] and acceptors give a further prove of the theoretical calculations.

FT-IR spectra of Schiff bases and their charge-transfer complexes

The infrared spectra of some Schiff bases prepared from 2-aminopyrazine were obtained as KBr discs. The most important absorption bands are registered in Table 2 and Fig. 1. The Schiff bases under investigation display the C=N band within the wavenumber range 1665-1590 cm^{-1}. The bands display within the wavenumber region 3360-3200 cm^{-1} are attributed to the stretching frequency of νCH bond in the heterocyclic moiety (pyrazine) which is in accordance with previous investigations.[42-45] The δCH bands are observed as two bands with varying intensities within the region 1458-1426 cm^{-1}. The γCH band of the CH=N group is in the wavenumber range 1002-994 cm^{-1}. The γCH bands of the aromatic rings are observed within the wavenumber range 832-748 cm^{-1}. The IR spectra of the formed complexes exhibit some drastic changes which are useful for elucidation of their molecular structures. These changes may be summarized as follows, the appearance of ν_{OH} band in the spectra of 3,5-dinitrosalicylic acid molecular complex with wavenumber 3570 and 3460 cm^{-1} may be designated to the carboxylic OH group. The $\nu_{C=O}$ bands of 3,5-dinitrosalicylic and 3,5-dinitrobenzoic acids shift to lower wavenumber on complex formation because of the π-π* electronic interaction. The two bands at 1700 and 1675 cm^{-1} assigned to C=O of the free 3,5-

DNSA and 3,5-DNBA appear as a single band within the wavenumber 1688 and1680 cm^{-1} in the spectra of the molecular complexes. Schiff bases are characterized by a weak band within the wavenumber range 1002-994 cm^{-1} which was assigned to the γCH (CH=N).[46] This band shifts to lower wavenumber on complex formation with PA, 3,5-DNSA and 3,5-DNBA, except for donor (p-$N(CH_3)_2$ where it is shifted to higher values. 2-aminopyrazine Schiff bases display the νCH asymmetric and νCH symmetric bands within the wavenumber 3215-3020 cm^{-1} and 3060-3020 cm^{-1}, respectively, Tables 3-6. On complex formation these bands are generally shifted to lower wavenumbers while the γCH bands of the Schiff bases are shifted to higher wavenumbers. This behaviour is ascribed to the decreased electron density on the donor molecule through π-π* electronic interaction resulting from the transfer of one electron for the HOMO of the donor to the LUMO on the acceptor molecules. This conclusion is strengthened by the general shift of the γCH bands of the heterocyclic ring of donors (2 adjacent H-atoms for pyrazine Schiff bases) to higher wavenumbers in contrast to those of the acceptor part which are shifted to lower wavenumbers. These shifts result from the decrease of electron density on the heterocyclic ring of the Schiff base and its increase on the acceptor molecule. One may deduce that the π-π* electron transfer originates from the heterocyclic ring to the acceptor molecule. In case of p-$N(CH_3)_2$ donor the benzal ring was the origin of CT.[47] The C=O bands of 3,5-DNSA and 3,5-DNBA are shifted to lower wavenumbers as a result of the raised electron density on the acceptor molecule. It is of interest to notice that in the case of 3,5-DNSA CT complex the two C=O bands of the free acceptor mostly appears as a single band. This is attributed to the rupture of the hydrogen bond existing in the free acceptor leading to the disappearance of rotational isomerism that take place in the free acceptor.[48] The CT complexes of pyrazine Schiff bases with 3,5-DNSA acceptor exhibit the νOH band within the wavenumber range 3250-3180 cm^{-1} which is assigned to the carboxylic OH group, Fig. S1. The NO_2 bands of the three acceptors used display some interesting behaviours which may be of great help for elucidation of the types of bonding in the CT complexes. In the case of complexes of picric acid, Fig. 2, the three ν asymmetric bands appear mostly as two bands due to the decreased diversity of the energy states of the NO_2 group. This results from the rupture of the intra-molecular hydrogen bond between the OH group and the neighboring NO_2 group. One of these two asymmetric NO_2 bands is shifted to higher wavenumber, while the second displays a counteract shift.

Table 2 Experimental, calculated and band assignments of infrared bands for 2-aminopyrazine Schiff bases.

	Wavenumber cm^{-1}								
X		νC-H		νC=N	δC-H	νC-H	γC-H		
	het. (Exp.) Calc.	asym. (Exp.) Calc.	sym. (Exp.) Calc.	(Exp.) Calc.	(Exp.) Calc.	(Exp.) Calc.	CH=N (Exp.) Calc.	arom. (Exp.) Calc.	het. (Exp.) Calc.
H	(3200)	(3058b)	(2980)	(1590)	(1458w, 1426)	(1192s)	(994)	(748)	(917)
	3203	3050	2988	1592	1458, 1430	1190	988	755	931
p-$N(CH_3)_2$	(3360)	(3210)	(2940)	(1665)	(1444, 1438)	(1237)	(1002)	(832, 813)	(828)
	3271	3208	3020	1666	1458, 1430	1241	1020	813	860

View Article Online
DOI: 10.1039/D0NJ05397J

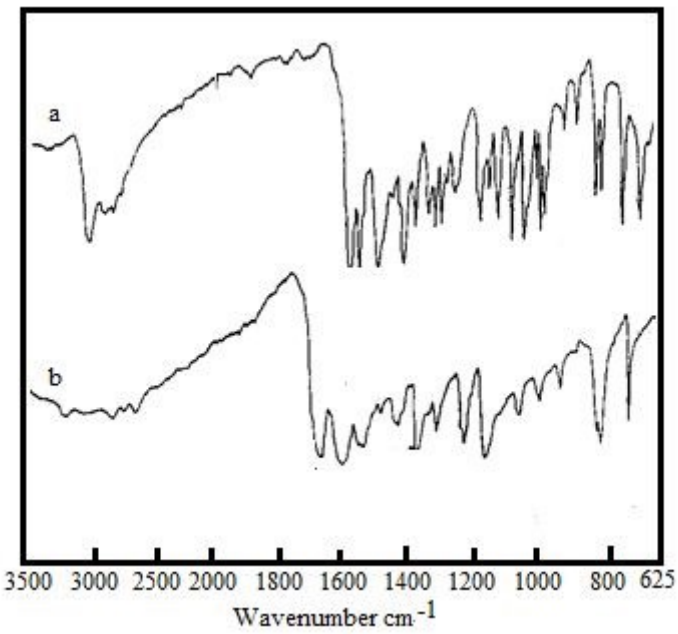

Fig. 1. FT-IR spectra of 2-aminopyrazine Schiff bases donors NBPA (a) and NDMABPA (b)

This may be justified by using the participation of the NO_2 group in position 4 in electronic interaction with the one nitrogen atom of the pyrazine moiety. The symmetric NO_2 bands are shifted to lower values and appear mostly as two peaks. In the case of 3,5-DNSA the orientation of the molecule permits the participation of only one nitro group in the n-π* electronic transition namely that in position 5 in the case of pyrazine Schiff base derivative. The ν symmetric bands exhibit a shift to lower wavenumbers in most cases. The

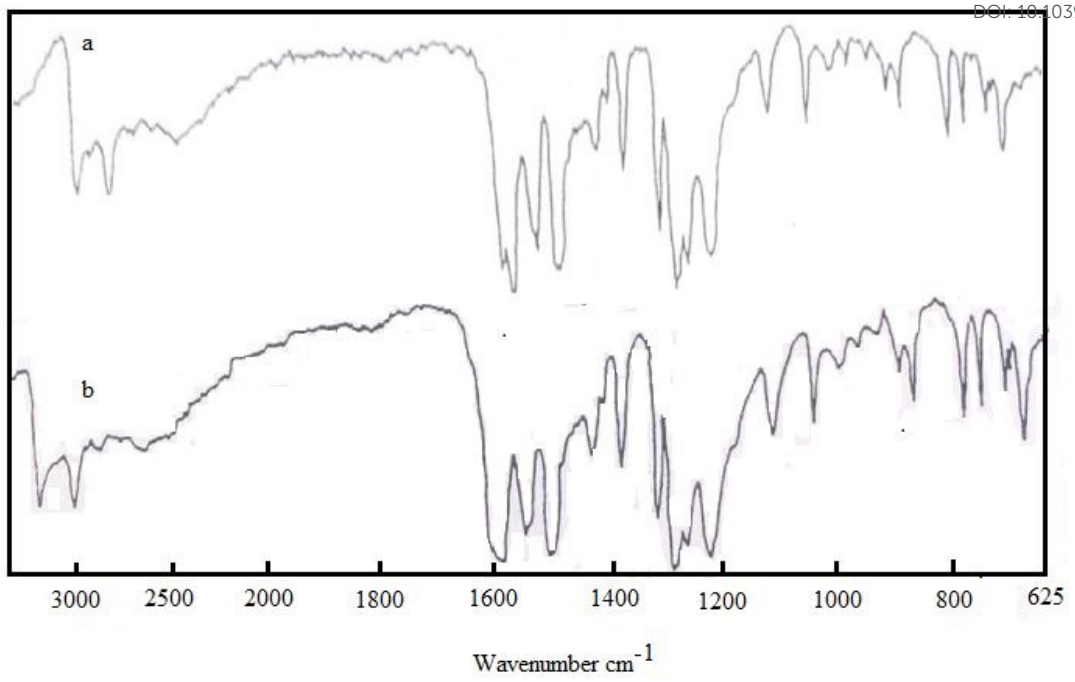

Fig. 2. FT-IR spectra of charge transfer complexes of 2-aminopyrazine Schiff bases donors NBPA (a) and NDMABPA (b) with Picric acid

asymmetric NO_2 bands of 3,5-DNBA, Fig. S2, display shifts to lower wavenumbers. This may be assigned to an intensified electron density on the acceptor molecule as a result of the π-π* electronic transition. The ν symmetric NO_2 bands exhibit similar behaviour.

Electronic absorption spectra of 2-aminopyrazine Schiff bases

The absorption spectra of Schiff bases derived from 2-aminopyrzine were scanned in ethanol and the values of λ_{max} and ε_{max} are listed in Table 7 and Fig. 3. Generally, all compounds exhibit an intense band within the wavelength 246-242 nm range, this may be assigned to the medium energy π-π* electronic transition within the benzene ring. For the unsubstituted compound (H), a shoulder is observed at 289 nm which may be attributed to π-π* electronic transition of the pyrazine ring and shifted to higher wavelength as a result of extended conjugation. The bands observed within the wavelength 348-326 nm in the CT complexes may be attributed to the π-π* electronic transition within the C=N linkage influenced by intramolecular charge-transfer.

Table 3 Main IR bands of CT complexes of 2-aminopyrazine with PA, 3,5-DNSA and 3,5-DNBA

Donor	Color	M.P. °C	νOH (Exp.) Calc.	C=O (Exp.) Calc.	νNO2 (Exp.) Calc.			γCH (Exp.) Calc.
					asym.	sym.	donor	acceptor
Complex of picric acid								
Free acceptor bands			(3110)		(1555, 1540, 1530)	(1350)		(784)
			3275		1535	1350		808
	Brownish white	225	(3430)	-	(1555, 1550)	(1340)	(812)	(783)
			3425		1550	1346	840	783
Complex of 3,5-dinitrosalicylic acid								
Free acceptor bands			(3570-3460)	(1700, 1675)	(1540, 1530)	(1349)	-	(925, 825)
			3721	1708	1515	1331		915
	Light yellow	210	(3380)	(1688)	(1538, 1520)	(1345)	(822)	(915, 810)
			3330	1672	1537	1342	827	915
Complex of 3,5-dinitrobenzoic acid								
Free acceptor bands			(3100)	(1707)	(1555, 1450)	(1350)		(923, 808)
			3268	1708	1502	1387		931
	Yellowish white	154	-	(1680)	(1545, 1535)	(1350)	(828)	(918, 800)
			-	1666	1543	1347	850	918

Table 4 Main IR bands of CT complexes of 2-aminopyrazine Schiff bases with picric acid

			Wavenumber cm^{-1}									
			Donor part							Acceptor part		
X	Color	M.P. °C		νC-H (Exp.) Calc.		C=N (Exp.) Calc.		γC-H ((Exp.) Calc.		NO_2 (Exp.) Calc.		γC-H (Exp.) Calc.
			het.	asym.	sym.		CH=N	arom.	het.	asym.	sym.	
Bands of free picric acid*										(1555, 1540, 1530)	(1350)	(784)
										1535	1350	771
H	Yellow	>240	(3378)	(3199)	(3060)	(1648)	(980sh)	(772)	(825)	(1560, 1550)	(1350, 1342)	(750)
			3425	3200	3034	1646	987	779	840	1542	1349, 1346	756
p-$N(CH_3)_2$	Brown yellow	231	(3358)	(3178)	(3040)	(1640)	(923)	(850)	(813)	(1559, 1550)	(1339, 1330)	(738)
			3383	3178	3042	1638	925	856	803	1565	1339, 1331	732

*νOH = 3110 cm^{-1}

Table 5 Main IR bands of CT complexes of 2-aminopyrazine Schiff bases with 3,5-dinitrosalicylic acid

			Wavenumber cm^{-1}									
			Donor part							Acceptor part		
X	Color	M.P. °C		νC-H		C=O		γC-H		NO_2		γC-H
			het.	asym.	sym.		CH=N	arom.	het.	asym.	sym.	
			(Exp.)	(Exp.)	(Exp.)	(Exp.)	(Exp.)	(Exp.)	(Exp.)	(Exp.)	(Exp.)	(Exp.)
			Calc.	Calc.	Calc.	Calc.	Calc.	Calc.	Calc.	Calc.	Calc.	Calc.
Bands of free 3,5-dinitrosalicylic acid*							(1700)			(1540, 1530)	(1349)	(925)
							1710			1516	1331	915
H	Light yellow	210	(3340)	(3120)	(3020)	(1690)	(998sh)	(785)	(825)	1545, 1530, 1525)	(1350)	(917)
			3330	3215	3021	1700	997	784	837	1537	1351	915
p-$N(CH_3)_2$	Brownish yellow	129	(3384)	(3086)	(3020)	(1687)	(899)	(820)	(820)	(1544s, 1534sh)	(1350)	(920)
			3358	3081	3023	1699	906	809	809	1542	1348	9018

*νOH = 3570, 3460 cm^{-1},

Table 6 Main IR bands of CT complexes of 2-aminopyrazine Schiff bases with 3,5-dinitrobenzoic acid

			Wavenumber cm^{-1}									
			Donor part							Acceptor part		
X	Color	M.P. °C		νC-H		C=O		γC-H		NO_2		γC-H
			het.	Asym.	sym.		CH=N	arom.	het.	asym.	sym.	
			(Exp.) Calc.	(Exp.) Calc.	(Exp.) Calc.	(Exp.) Calc.	(Exp.) Calc.	(Exp.) Calc.	(Exp.) Calc.	(Exp.) Calc.	(Exp.) Calc.	(Exp.) Calc.
Bands of free 3,5-dinitrobenzoic acid*							(1707)	(725)	(811)	(1555, 1540)	(1350)	(923)
							1708	744	811	1502	1387	931
H	Light brown	151	(3350)	(3100)	(3040)	(1675)	(982sh)	(799)	(830)	(1550, 1545, 1540)	(1370)	(925)
			3303	3187	3036	1666	984	810	850	1543	1378	934
p-$N(CH_3)_2$	reddish orange	107	(3280)	(3100)	(3050)	(1690)	(982sh)	(860)	(815)	(1550, 1540)	(1345)	(920)
			3283	3093	3038	1697	996	850	810	1544	1354	919

*νOH = 3100 cm^{-1}

View Article Online
DOI: 10.1039/D0NJ05397J

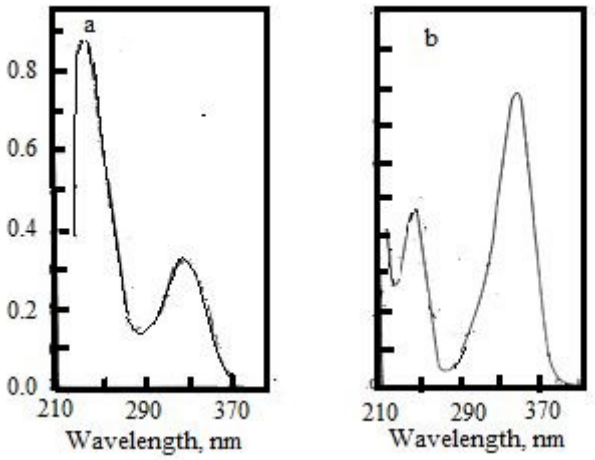

Fig. 3. Electronic absorption spectra of 2-aminopyrazine Schiff bases NBPA (a) and NDMABPA (b) in ethanol

Ionization potential of 2-aminopyrazine Schiff bases

The amounts of the ionization potential (Ip) of the free donors are determined from their electronic spectra applying the relation: $Ip = a + b\ \nu_o$, where ν_o is the energy of the HOMO-LUMO π-π^* transition of the donor in the gas phase taken, a and b are constants amounting to 5.11 and 0.701,[49] Table 8. The value of experimental E_{CT} can be calculated from λ_{max} of electronic spectra applying the following equation[50]:

$$E_{CT} = 1239.9/\lambda_{CT}\ \text{nm} \quad \text{eV}$$

The results are recorded in Table 8. It is apparent that the Schiff base with electron donating group has lower ionization potential value than that with electron withdrawing group.

Charge-transfer complexes with PA, 3,5-DNSA and 3,5-DNBA acceptors

This group comprises complexes formed with PA, 3,5-DNSA and 3,5-DNBA when mixed with the donor in the molecular ratio 1:1. The fact that such acceptors have strong acidic character is supported by their low ionization constant (pK) values accounting to 1.60 and 2.82[51] for picric and 3,5-dinitrobenzoic acids and $pK_1 = 2.94$, $pK_2 = 9.94$[52] for 3,5-dinitrosalicylic acid, respectively. The donors under investigation possess more than one basic center in the molecule. Hence, an acid-base interaction is expected to take place. These complexes are characterized by their relatively high melting points (Tables 3-6).

View Article Online
DOI: 10.1039/D0NJ05397J

Electronic absorption spectra of charge-transfer complexes

The electronic absorption spectra of CT complexes formed between picric acid and the prepared Schiff bases were investigated applying the nujol mull technique. The spectra display new very broad bands located at the longer wavelength side which were not observed in the absorption spectra of either the donors (Schiff bases) or the acceptor (picric acid). These bands may be due to the intermolecular CT interaction between the donor and acceptor molecules, Fig. 4. For the verification of this postulation, the E_{CT} values were analyzed from the absorption spectra utilizing the above equation.[47] The theoretical E_{CT} values were also calculated using Briegleb equation:[53]

$$E_{CT} = Ip - (E_A + C)$$

Where Ip is the ionization potential of the donor as calculated in Table 8, E_A is the electron affinity of the acceptor = 0.7 eV and C is the coulomb force taken as 4.7 eV.[48] The λ_{max} nm and E_{CT} values (observed and calculated) are depicted in Table 9. The values of E_{CT} obtained from the absorption spectra are nearly concordant with those calculated which is in favor for

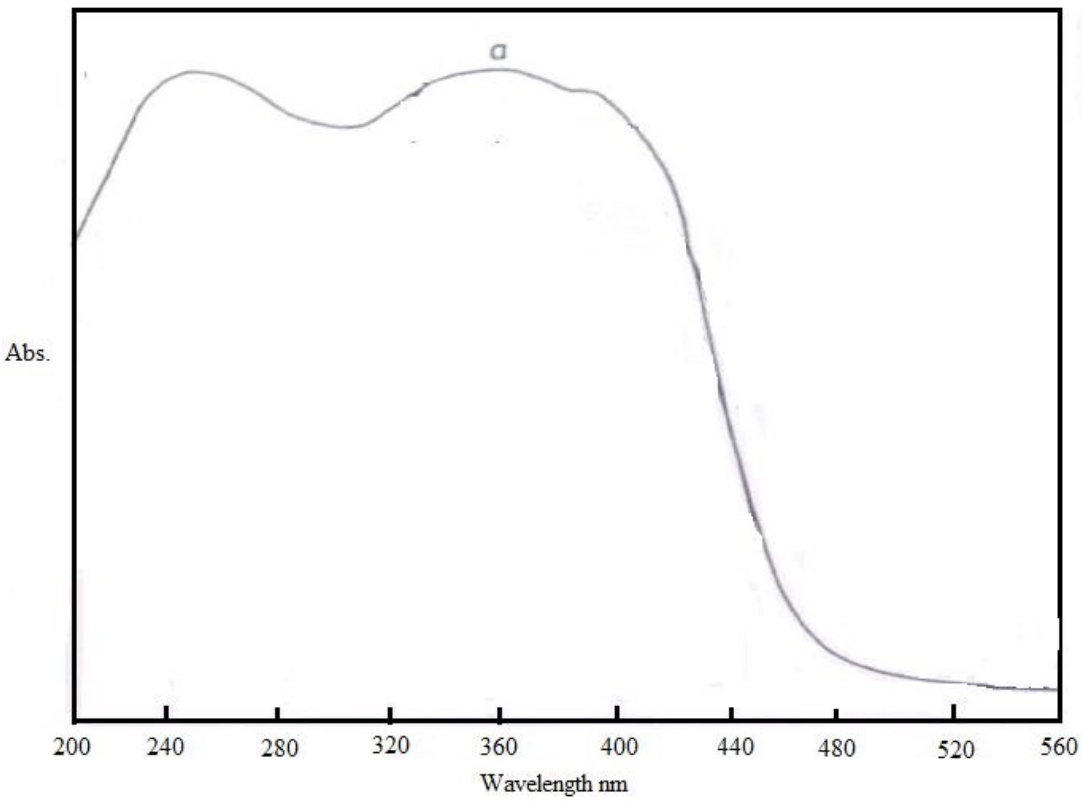

Fig. 4. Electronic absorption spectra of CT complex of 2-aminopyrazine Schiff base with picric acid

Table 7 Absorption bands of 2-aminopyrazine Schiff bases in ethanol and its CT complex with picric acid

X	π-π*		π-π* pyrazine		CT		E_{CT} eV	
	λ_{max} nm	ε_{max} x10^{-4}	λ_{max} nm	ε_{max} x10^{-4}	λ_{max} nm	ε_{max} x10^{-4}	λ_{max} nm	Obs.	Calc.
H	242	2.90	289 sh	0.55	326	1.08	390	3.18	2.38
p-$N(CH_3)_2$	246	1.60	-	-	348	2.67	420	2.95	2.21

Table 8 Calculated values of ionization potential of 2-aminopyrazine Schiff bases

X	CT		Ip
	λ_{max} nm	E_{CT}	a=5.11, b=0.701
H	326	3.81	7.78
p-$N(CH_3)_2$	348	3.57	7.61

their assignment as CT bands. The CT band observed have a composite nature, this may be considered as a further support for the existence of another interaction, i.e. n-π*, besides the π-π* electronic interaction. However, no clear band is observed which can be assigned to the n-π* interaction.

Table 9 Electronic absorption bands of CT complexes of 2-aminopyrazine Schiff bases with picric acid

X	λ_{max} nm	E_{CT} eV	
		Obs.	Calc.
H	390	3.18	2.38
p-N$(CH_3)_2$	420	2.95	2.21

^{1}H-NMR spectrum of charge-transfer complex of 2-aminpyrazine Schiff base with picric acid

The NMR spectrum of CT complex of 2-aminopyrazine Schiff bases with picric acid was investigated and compared to that of the free component. The NMR spectrum of picric acid displays the aromatic proton signals at 8.30 and 8.40 ppm and that of OH at 6.16 ppm as shown in Scheme 2 and Table 10. A comparison between the NMR spectra of the CT complex and that of the component reveals that the signals of the acceptors are shifted to higher field values while that of the donors are displayed to lower fields, Table 10 and Fig. 5. This results from the π-π* electronic interaction leading to the increased π-electron density on the acceptor and its decrease on the donor molecule.

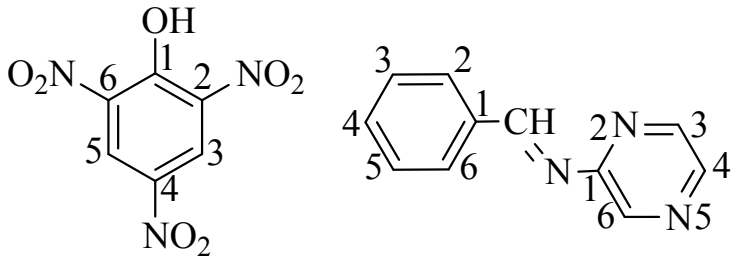

Scheme 2. Numbering system of picric and 2-aminpyrazine Schiff base

View Article Online
DOI: 10.1039/D0NJ05397J

Table 10 ^{1}H-NMR signals of picric, 2-aminpyrazine Schiff base and its CT complex with picric acid

Compound	Acceptor part							Donor part			
	H^2	H^3	H^4	H^5	H^6	CH	OH	H^3	H^4	H^5	H^6
Picric acid	-	8.30	-	8.40	-	-	6.16	-	-	-	-
	-	*8.46	-	*8.46	-	-	*6.16				
2-aminopyrazine Schiff base (H)				Signals of benzal ring					Signals of hetero ring		
	7.60	7.50	8.36	7.50	7.60	9.7	-	8.35	8.70	-	8.70
CT complex with picric acid	8.70	8.70	8.70	8.70	8.70	9.00	-	8.15	7.05		8.67

*After complex formation

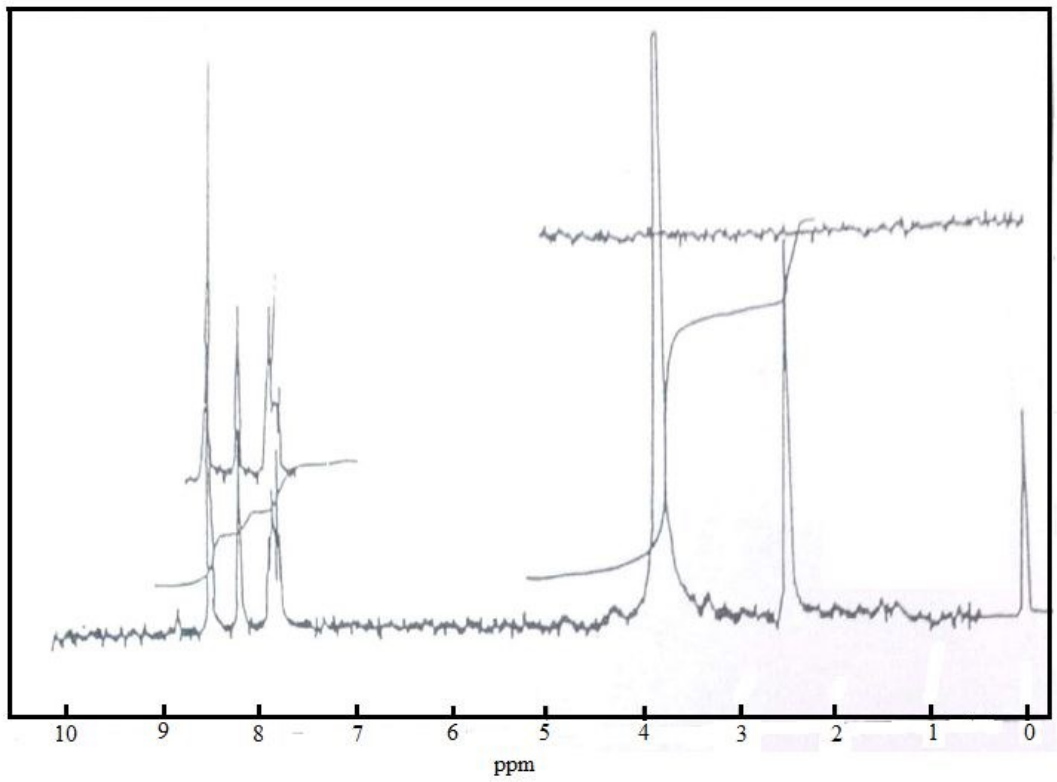

Fig. 5. ^{1}H NMR of spectrum of CT complex of 2-aminopyrazine Schiff base NBPA with picric acid

View Article Online
DOI: 10.1039/D0NJ05397J

Computational DFT Analysis

Density functional theory examination was done according to Becke's three parameter gradient-corrected exchange potential and the Lee-Yang-Parr Gradient-corrected correlation potential (B3LYP), and significant calculations were achieved by using 6-311G** basis set. This model has been extensively used for geometry optimization and the purpose of electronic properties. The optimized amounts of bond lengths, bond angles, molecular electrostatic potential map values, characterization of the frontier molecular orbital[54] surfaces and natural atomic charges were produced. Gauss-View 5.0 and Chemcraft programs have been exploited to achieve the calculated results, and visualize the optimized structures, the frontier molecular orbitals and molecular electrostatic potential maps. The optimized geometries of NBPA and NDMABPA Schiff bases (donors); picric (PA), 3,5-dinitrosalicylic (3,5-DNSA) and 3,5-dinitrobenzoic (3,5-DNBA) acids (acceptors) and their CT complexes with numbering system are shown in Fig. 6.

Molecular orbital treatment

Geometry of the donors, acceptors and CT complexes

The optimized bond lengths, recorded in Table 11 and Fig.6, show that the carbon nitrogen bond length of picric acid (PA) in CT complex C25-N34 of the picric acid moieties of the complex increased to 1.480 Å compared with 1.467 Å for free picric acid (PA), in case of 3,5-dinitrosalicylic acid (3,5-DNSA) acceptor, the bond length C28-N36 in the CT complex increases from 1.464 Å to 1.472 Å associated to free 3,5-DNSA while for 3,5-DNBA, the bond length C27-N34 in the CT complex also increases from 1.486 Å to 1.491 Å related to free 3,5-DNBA. This result indicates that the bond length of the carbon-nitrogen bond in PA, 3,5-DNSA and 3,5-DNBA increases, thus confirming the electron transfer from the labile lone pair of electrons of the 2-aminopyrazine Schiff donor (-N=CH) nitrogen towards the carbon-nitrogen bond of PA, 3,5-DNSA and 3,5-DNBA acceptors. It is important to notice that the nitrogen of 2-aminopyrazine Schiff base donor was found to be oriented towards the PA, 3,5-DNSA and 3,5-DNBA acceptors and this orientation produced the resonating structure from the electron transfer to the PA, 3,5-DNSA and 3,5-DNBA acceptors of the CT complex. The bond lengths of PA, 3,5-DNSA and 3,5-DNBA decrease in the CT complex as compared to themselves. This indicates the transfer of π-electron from the HOMO of 2-aminopyrazine Schiff base donors to the π* LUMO of PA, 3,5-DNSA and 3,5-DNBA

moieties. The C6-N7 and C8-N7 bond lengths of the CT complex decreased to 1.279 Å and 1.394 Å compared with 1.282 Å and 1.402 Å, from 1.402 Å and 1.282 Å to 1.398 Å and 1.278 Å, from 1.402 Å and 1.282 Å to 1.395 Å and 1.279 Å of free PA, 3,5-DNSA and 3,5-DNBA acceptors, respectively. These results in the expansion of bond lengths because of the increase of electron density of acceptor in the complex compared to free acceptor. It indicates that the electron density on the donor moiety of the complex decreases, which results in the contraction of bond lengths compared to donor alone. The CT complex is further confirmed from the changes in its bond angles as compared to the reactants as presented in Table 11. The free acceptor can be further confirmed from the decreasing bond angles of C2-N13-O18 and C2-N13-O19 of the CT complex (from 117.728° to 116.749° and from 118.825° to 116.811°), C28-N36-O38 from 119.091° to 118.014° and C25-C27-N34 from 118.873 to 118.813 of free PA, 3,5-DNSA and 3,5-DNBA acceptors, respectively. Moreover, the bond angle of C24-C25-N34 decreases to 119.022° compared to 120.403° of picric acid acceptor. In the case of 2-aminopyrazine Schiff base donor, the bond angle N4-C6-N7 decreases from 121.811° to 117.111°, 117.216°, 117.118° in the CT complexes as compared to the donor alone which confirms the π-π* transition from HOMO to LUMO molecular orbitals of the characterized CT complex. In case of p-N-dimethyl-2-aminopyrazine Schiff base donor, the optimized bond lengths, recorded in Table S1 and Fig. 6, show that the carbon nitrogen bond length of picric acid (PA) in CT complex C33-N44 of the picric acid moieties of the complex increased to 1.473 Å compared with 1.467 Å for free picric acid, in case of 3,5-DNSA acceptor, the bond length C26-N38 in the CT complex increases from 1.464 Å to 1.471 Å associated to free 3,5-DNSA while for 3,5-DNBA, the bond length C26-N33 in the CT complex also increases from 1.486 Å to 1.491 Å related to free 3,5-DNBA. These results indicate that the bond length of the carbon-nitrogen bond in PA, 3,5-DNSA and 3,5-DNBA increases thus confirming the electron transfer from the labile lone pair of electrons of the p-N-dimethyl-2-aminopyrazine Schiff donor (-N=CH) nitrogen towards the carbon-nitrogen bond of PA, 3,5-DNSA and 3,5-DNBA acceptors. It is important to note that the nitrogen of p-N-dimethyl-2-aminopyrazine Schiff donor was found to be oriented towards the PA, 3,5-DNSA and 3,5-DNBA acceptors and this orientation produced the resonating structure from the electron transfer to the PA, 3,5-DNSA and 3,5-DNBA acceptors of the CT complex. The bond lengths of PA, 3,5-DNSA and 3,5-DNBA decrease in the CT complex as compared to themselves. This indicates the π-electron transfer from the HOMO of

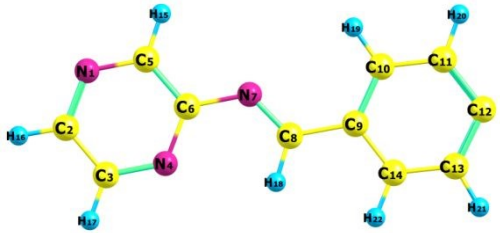

Donor (NBPA)

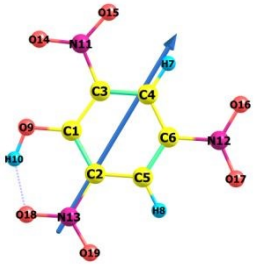

Acceptor (PA)

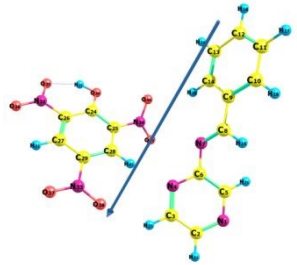

CT complex

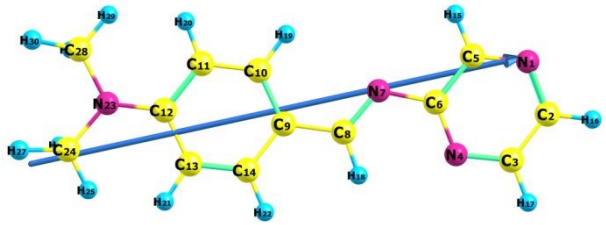

Donor (NDMABPA)

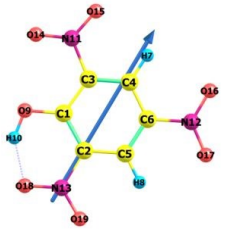

Acceptor (PA)

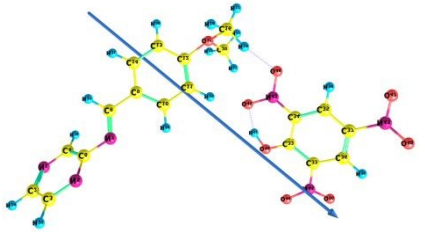

CT complex

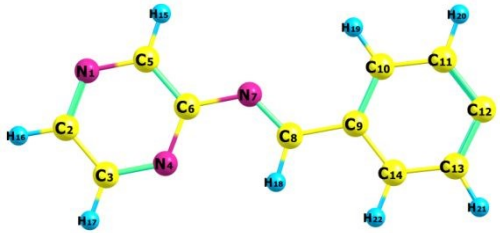

Donor (NBPA)

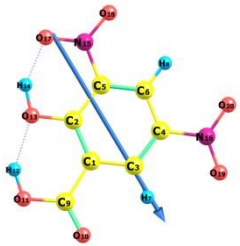

Acceptor (3,5-DNSA)

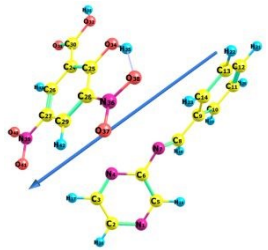

CT complex

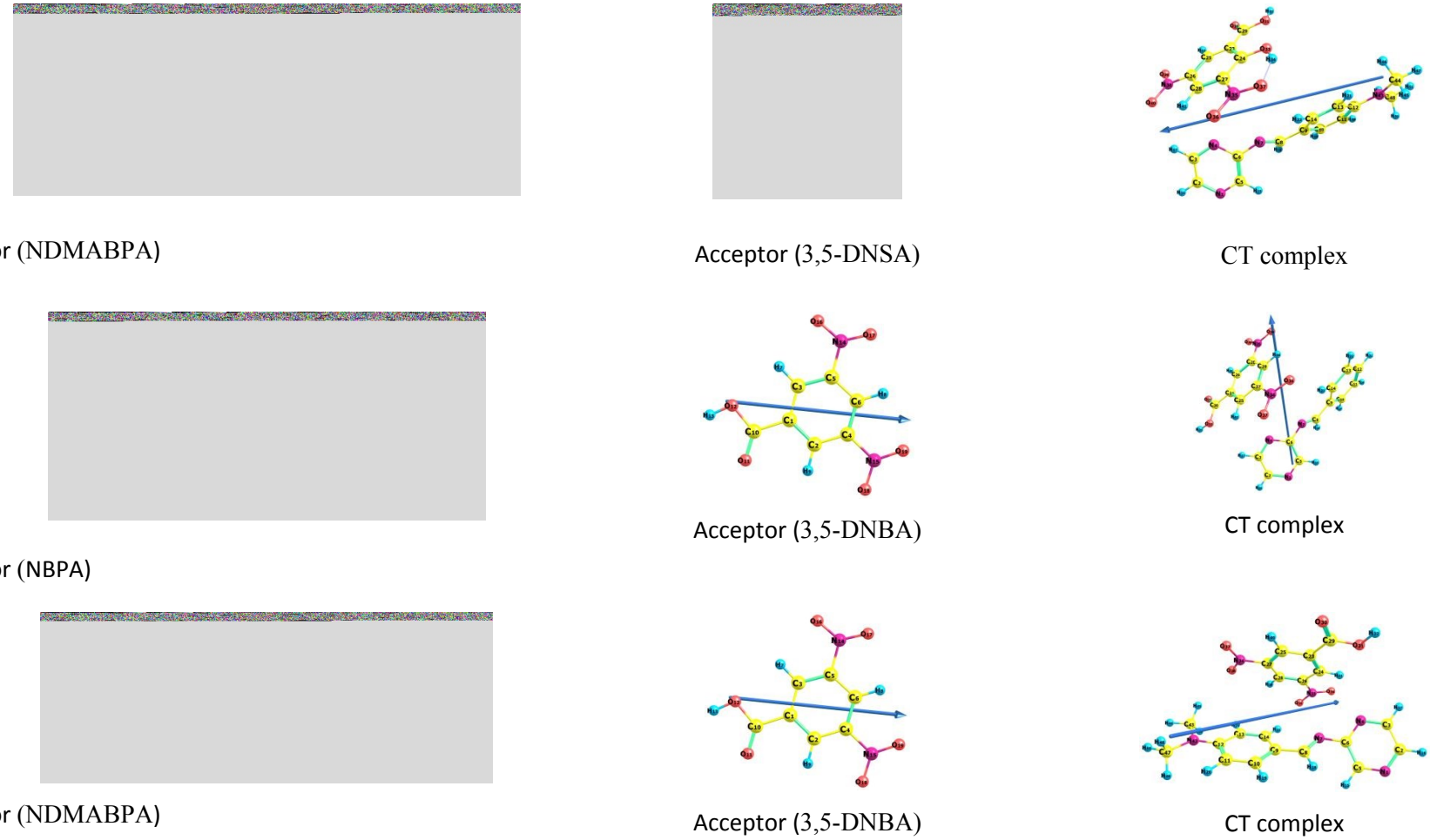

Fig. 6 Optimized geometry, numbering system, and vector of dipole moment for the studied 2-aminopyrazine, (p-N$(CH_3)_2$-2-aminopyrazine Schiff bases (donors); Picric, 3,5-dinitrosalicylic and 3,5-dinitrobenzoic acids (acceptors) and their charge transfer complexes using B3LYP/6-311G**

p-N-dimethyl-2-aminopyrazine Schiff donor to the π* LUMO of PA, 3,5-DNSA and 3,5-DNBA moieties. The C6-N7 and C8-N7 bond lengths of the CT complex of PA, 3,5-DNSA and 3,5-DNBA acceptors, respectively decreased to 1.272 Å and 1.381 Å compared with 1.435 Å and 1.396 Å, from 1.396 Å and 1.288 Å to 1.393 Å and 1.285Å, from 1.396 Å and 1.288 Å to 1.391 Å and 1.285 Å of free donor. These results in the expansion of bond lengths because of the rise of electron density of acceptor in the complex compared to free acceptor. It indicates that the electron density on the donor moiety of the complex decreases, which results in the contraction of bond lengths compared to donor alone. The CT complex is further confirmed from the changes in its bond angles as compared to the reactants as presented in Table S1. The free acceptor can be further confirmed from the decreasing bond angles of C2-N13-O18 and C2-N13-O19 of the CT complex (from 117.728° to 116.752° and from 118.825° to 118.411°), C26-N38-O39 from 117.593° to 117.568° and C26-N38-O40 from 119.091 to 117.500 of free PA, 3,5-DNSA and 3,5-DNBA acceptors, respectively. Moreover, the bond angle of C24-C27-N35 decreases to 120.855° compared to 122.269° of 3,5-DNSA acceptor. In the case of p-N-dimethyl-2-aminopyrazine Schiff base donor, the bond angle N4-C6-N7 decreases from 122.385° to 116.574°, 117.375° and 117.061° in the CT complexes as compared to the donor alone which confirms the π-π* transition from HOMO to LUMO molecular orbitals of the characterized CT complexes.

Global reactivity descriptors

Frontier molecular orbital energies calculation for CT complexes

Molecular orbital analysis shows that the frontier molecular orbitals are mainly composed of N atomic orbitals. HOMO-LUMO calculation of 2-aminopyrazine and p-N-dimethyl-2-aminopyrazine Schiff bases donors and PA, 3,5-DNSA and 3,5-DNBA acceptors, the complexes in the ground state are obtained by the DFT method with basis sets B3LYP/6-311G** and presented in Figs. 7-9. It is clear from the figure that the HOMOs are mainly delocalized on the donor moiety (2-aminopyrazine and p-N-dimethyl-2-aminopyrazine Schiff bases), while the LUMOs are localized on acceptors PA, 3,5-DNSA and 3,5-DNBA. The molecular orbital HOMO is localized on the 2-aminopyrazine and p-N-dimethyl-2-aminopyrazine Schiff bases part of the complex and particularly on the N atomic orbital. Thus, one concludes that the n-electrons are localized in HOMO molecular orbital. The other molecular orbitals are located on the p orbitals of the benzene moieties of 2-aminopyrazine and p-N-dimethyl-2-aminopyrazine Schiff bases in the CT complexes, the HOMO can be

considered as π molecular orbitals and the LUMO as the π* molecular orbital. Consequently, the noticed transitions can be ascribed to n–π* and π–π* transitions. The energy values for HOMO's and LUMO's of donors, acceptors and donor-acceptor complexes in the ground state are provided in Table 12 and it is interesting to note from Table 12, that in case of 2-aminopyrazine Schiff base, the LUMO energy level of the donor-acceptor CT complexes (-0.1381, -0.1337 and -0.1230 a. u.) compares well with the LUMO energy level of acceptors (-0.1506, -0.1610 and -0.1352 a. u.) while the HOMO energy (-0.2506, -0.2566 and -0.2567 a. u.) level of the CT complex are close to HOMO energy level of 2-aminopyrazine Schiff base donor. In Figs. 2-4, some frontier orbitals are exhibited. The reason for localized frontier molecular orbitals of donor-acceptor complex system is like other electron donor-acceptor aggregate systems. Hence, the orbital interaction energy arises mainly due to the CT concerning occupied and unoccupied orbitals. The energy difference between the HOMO and LUMO, E_g, of the studied CT complexes occurs in the range 3.35-3.30 eV. The energy gap for 3,5-DNSA CT complex is the maximum (3.35 eV) while 3,5-DNBA CT complex has the minimum (3.30 eV) value. As a result, charge-transfer and polarization can easily occur within the 3,5-DNBA CT complex than other complexes with more reactivity. The chemical hardness, η, electronegativity, χ, chemical potential, π, and global softness, S, were calculated using HOMO and LUMO energies and listed in Table 12. PA complex has the lowest η and maximum S values which means that the CT occurs easily in this complex and has a smaller chemical hardness. It can be decided that the large E_g gap indicates a hardness of the molecule, while smaller E_g gap is a characteristic for a soft and reactive molecule. The electron affinity values of the CT complexes have the order: < 3,5-DNSA < 3,5-DNBA < PA. Therefore, CT and polarization can easily occur within the PA complex than the other complexes due to its higher reactivity. The computed reactivity parameters shown in Table 12 reveal that PA complex has the lowest η and maximum S values which means that the CT occurs in this CT complex and has softer chemical hardness. It is interesting to note from Table S2, that in case of p-N-dimethyl-2-aminopyrazine Schiff base, the LUMO energy level of the donor-acceptor CT complexes (-0.1182, -0.1249 and -0.1217 a. u.) compares well with the LUMO energy level of acceptors (-0.1506, -0.1610 and -0.1352 a. u.) while the HOMO energy (-0.1652, -0.2135 and -0.2107 a. u.) level of the CT complex are close to HOMO energy level of p-N-dimethyl-2-aminopyrazine Schiff base donor. The energy difference between the HOMO and LUMO, E_g, of the studied CT complexes occurs in the range 2.42-

Table 11 Selected geometric bond lengths, bond angles and dihedral angles of the optimized 2-aminopyrazine Schiff base (donor), Picric (PA), 3,5-dinitrosalicylic (3,5-DNSA) and 3,5-dinitrobenzoic (3,5-DNBA) acids (acceptors) and their CT complexes using B3LYP/6-311***

Ligand/CT complexes	Bond lengths (Å)		Bond angles		Dihedral angles	
Donor (NBPA)	C5-C6	1.404	N1-C5-C6	120.111	C5-C6- N7-C8	180.000
	C6-N4	1.371	C5-C6-N4	117.937	C6- N7-C8-C9	180.000
	C6-N7	1.435	C5-C6-N7	120.252	N7-C8-C9-C10	0.000
`	N7-C8	1.296	N4-C6-N7	121.811	N7-C8-C9-C14	180.000
	C8-C9	1.503	N7-C8-C9	124.074	N4-C6-N7-C8	0.000
	C9-C14	1.398	C8-C9-C10	124.719		
	C9-C10	1.407	C8-C9-C14	117.667		
			C10-C9-C14	117.615		
Acceptor (PA)	C1-C2	1.428	O9-C1-C2	122.861	O9-C1-C2-C5	180.000
	C2-C5	1.387	C1-C2-N13	120.403	C1-C2-N13-O18	0.000
	C2-N13	1.467	C2-N13-O18	117.728	C1-C2-N13-O19	180.000
	N13-O18	1.244	C2-N13-O19	118.825	O9-C1-C3-N11	0.000
	N13-O19	1.212	N13-C2-C5	30.603	C1-C3-C4-C6	0.000
			O9-C1-C3	121.521	N13-C2-C5-C6	-180.000
CT complex	C8-N7	1.279	N4-C6-N7	117.111	N4-C6-N7-C8	136.781
	C6-N7	1.394	C5-C6-N7	122.368	C6-N7-C8-C9	174.955
	C6-N4	1.339	C6-N7-C8	28.813	N1-C5-C6-N7	-179.496
	C8-C9	1.464	N7-C8-C9	123.493	N4-C6-N7-N34	-35.783
	C25-N34	1.480	C24-C25-N34	119.022	N34-C25-C24-O30	2.271
	C24-C25	1.413	C25- N34-O39	116.749	N34-C25-C28-C29	178.952
	C24-O30	1.319	C25- N34-O40	116.811		
	C25-C28	1.379				

Acceptor (3,5-DNSA)						
	C2-C5	1.417	C2-C5-C6	121.715	C1-C2-C5-N15	-179.987
	C5-C6	1.389	C2-C5-N15	120.693	C2-C5-N15-O17	0.011
	C5-N15	1.464	C5-C2-O13	122.269	C2-C5-N15-O18	-179.980
	C2-O13	1.337	C5-N15-O17	117.593	O13-C2-C5-N15	0.023
	N15-O17	1.247	C5-N15-O18	119.091	C6-C5-N15-O17	179.983
	N15-O18	1.211			C6-C5-N15-O18	0.026
CT complex	C6-N7	1.398	N4-C6-N7	117.216	C3-N4-C6-N7	-178.675
	C8-N7	1.278	C6-N7-C8	119.169	N4-C6-N7-C8	-136.770
	C8-C9	1.466	C5-C6-N4	120.722	C6-N7-C8-C9	-174.022
	C6-N4	1.342	C5-C6-N7	121.947	N4-C6-N7-N36	29.943
	C5-C6	1.413	N7-C8-C9	123.554	C9-C8-N7-N36	23.662
	C9-C10	1.406	C8-C9-C10	118.851	C8-N7-N36O37	-149.644
	C9-C14	1.408	C8-C9-C14	121.836	C8-N7-N36O38	-26.922
	N36-O37	1.221	C6-N7-N36	105.766	C25-C28-N36-O38	-3.414
	N36-O38	1.255	O37-N36-O38	122.752	O34- C25-C28-N36	0.568
	C28-N36	1.472	C28-N36-O37	119.231	C24-C25-C28-N36	-179.213
	C25-C28	1.429	C28-N36-O38	118.014	C27-C29-C28-N36	179.607
	C28-C29	1.391	C25-C28-N36	121.087	C29-C28-C25-O34	-178.799
	C25-O34	1.324	C28-C25-O34	122.604		
			C25-C28-C20	122.137		
Acceptor (3,5-DNBA)						
	C3-C5	1.389	C3-C5-C6	122.546	C1-C3-C5-N14	180.000
	C5-C6	1.387	C3-C5-N14	118.873	C4-C6-C5-N14	180.000
	C5-N14	1.486	C6-C5-N14	118.581	C3-C5-N15-O16	0.000
	N14-O16	1.221	C5-N14-O16	117.168	C3-C5-N15-O17	180.000

	N14-O17	1.2205	C5-N14-O16	117.229		
CT complex						
	C3-N4	1.333	N4-C6-N7	117.118	C3-N4-C6-N7	-179.228
	N4-C6	1.338	C6-N7-C8	119.416	N4-C6-N7-C8	-135.375
	C5-C6	1.410	C5-C6-N4	120.609	C6-N7-C8-C9	-175.142
	C6-N7	1.395	C5-C6-N7	122.188	N4-C6-N7-N35	37.539
	N7-C8	1.279	C8-C9-C10	118.845	C8-N7-N34O36	-29.370
	C8-C9	1.464	C8-C9-C14	121.781	C8-N7-N34O37	-154.720
	N7-N34	3.506	O36-N34-O37	125.273	C29-C27-N34-O36	-4.017
	N34-O36	3.506	C25-C27-N34	118.813	C29-C27-N34-O37	175.210
	N34-O37	1.224	C27-N34-O37	117.514	C24-C25-C27-N34	179.595
	C27-N34	1.491	C25-C27-C29	122.529	C28-C29-C27-N34	-179.633
	C25-C27	1.388				
	C27-C29	1.386				

View Article Online
DOI: 10.1039/D0NJ05397J

1.28 eV. The energy gap for 3,5-DNBA CT complex is the maximum (2.42 eV) while PA CT complex has the minimum (1.28 eV) value. As a result, CT and polarization can easily occur within the PA CT complex than other complexes with more reactivity. The chemical hardness, η, electronegativity, χ, chemical potential, π, and global softness, S, were calculated using HOMO and LUMO energies and listed in Table S2. PA CT complex has the lowest η and maximum S values which means that the charge-transfer occurs easily in this complex and has a lesser chemical hardness. It can be concluded that the large E_g gap indicates a hardness of the molecule, while smaller E_g gap is representative for a soft and reactive molecule. The electron affinity values of the CT complexes have the order: < PA < 3,5-DNBA < 3,5-DNSA. Therefore, CT and polarization can easily occur within the 3,5-DNSA complex than other complexes as a result of its higher reactivity. The computed reactivity parameters shown in Table S2 reveal that 3,5-DNSA complex has the lowest η and maximum S values which means that the CT occurs in this CT complex and has lower chemical hardness.

Natural charges and natural population

The Natural atomic charges perform a fundamental role in the consequence of quantum mechanical computations to the molecular systems. The comparison of natural charge distribution of the donor (2-aminopyrazine Schiff base), acceptors (PA, 3,5-DNSA and 3,5-DNBA) and CT complex (donor-acceptor) are shown in Table 13. The increase in the negative charges on the atoms of acceptor moieties suggests that the CT from the donor to PA, 3,5-DNSA and 3,5-DNBA acceptors. A large increase was observed on N34, N36 and N34, suggesting that the unoccupied molecular orbitals are contained on these atomic centres. It is also observed that the decrease of effective negative charge on N7 of the donor atom of the CT complex relative to free donor could be attributed to further supports the CT process from the donor to PA, 3,5-DNSA and 3,5-DNBA acceptors upon complexation. This information gives emphasis to that the natural atomic charges are important to explain the establishment of a CT complex between 2-aminopyrazine Schiff base donor and PA, 3,5-DNSA and 3,5-DNBA acceptors. It is evident from Table 13 that the electronic charge on N7 of the donor (2-aminopyrazine Schiff base) decreases in the CT complex formation

Table 12 Total energy, energy of HOMO and LUMO, energy gap, ionization energy (I, eV), electron affinity (A, eV), absolute electronegativities, (χ, eV), absolute hardness (η, eV), global softness (S, eV^{-1}) chemical potential (π, eV^{-1}) global electrophilicity (ω, eV), additional electronic charge, $\Delta N_{max,}$ of the studied 2-aminopyrazine Schiff base (donor), Picric, 3,5-dinitrosalicylic and 3,5-dinitrobenzoic acids (acceptors) and their CT complex usingB3LYP/6-311G(d,p)

Parameter	Donor	Acceptor	CT complex	Acceptor	CT complex	Acceptor	CT complex
	H	PA		3,5-dNSA		3,5-DNBA	
E_T, a.u.	-588.97	-921.20	-1510.18	-904.97	-1493.927	-829.85	-1418.70
E_{HOMO}, a.u.	-0.2426	-0.3117	-0.2506	-0.3129	-0.2566	-0.3280	-0.2567
E_{LUMO}, a.u.	-0.0869	-0.1506	-0.1381	-0.1610	-0.1337	-0.1352	-0.1230
E_g, eV	4.2352	4.3832	3.0624	4.1334	3.3465	5.2464	3.3038
I, eV	6.6013	8.4824	6.8189	8.5145	6.9836	8.9265	6.9839
A, eV	2.3661	4.0992	3.7566	4.3811	3.6371	3.6801	3.6801
χ, eV	4.4837	6.2908	5.2878	6.4478	5.3103	6.3033	5.3320
η, eV	2.1176	2.1916	1.5312	2.0667	1.6732	2.6232	1.6519
S, eV	0.2361	0.2281	0.3265	0.2419	0.2988	0.1906	0.3027
π eV	-4.4837	-6.2908	-5.2877	-6.4478	-5.3103	-6.3033	-5.3320
(ω, eV)	4.7468	9.1353	9.1300	10.0566	8.4268	12.2387	8.6053
$\Delta N_{max.}$	2.1173	2.8704	3.4533	3.1198	3.1737	2.4029	3.4138

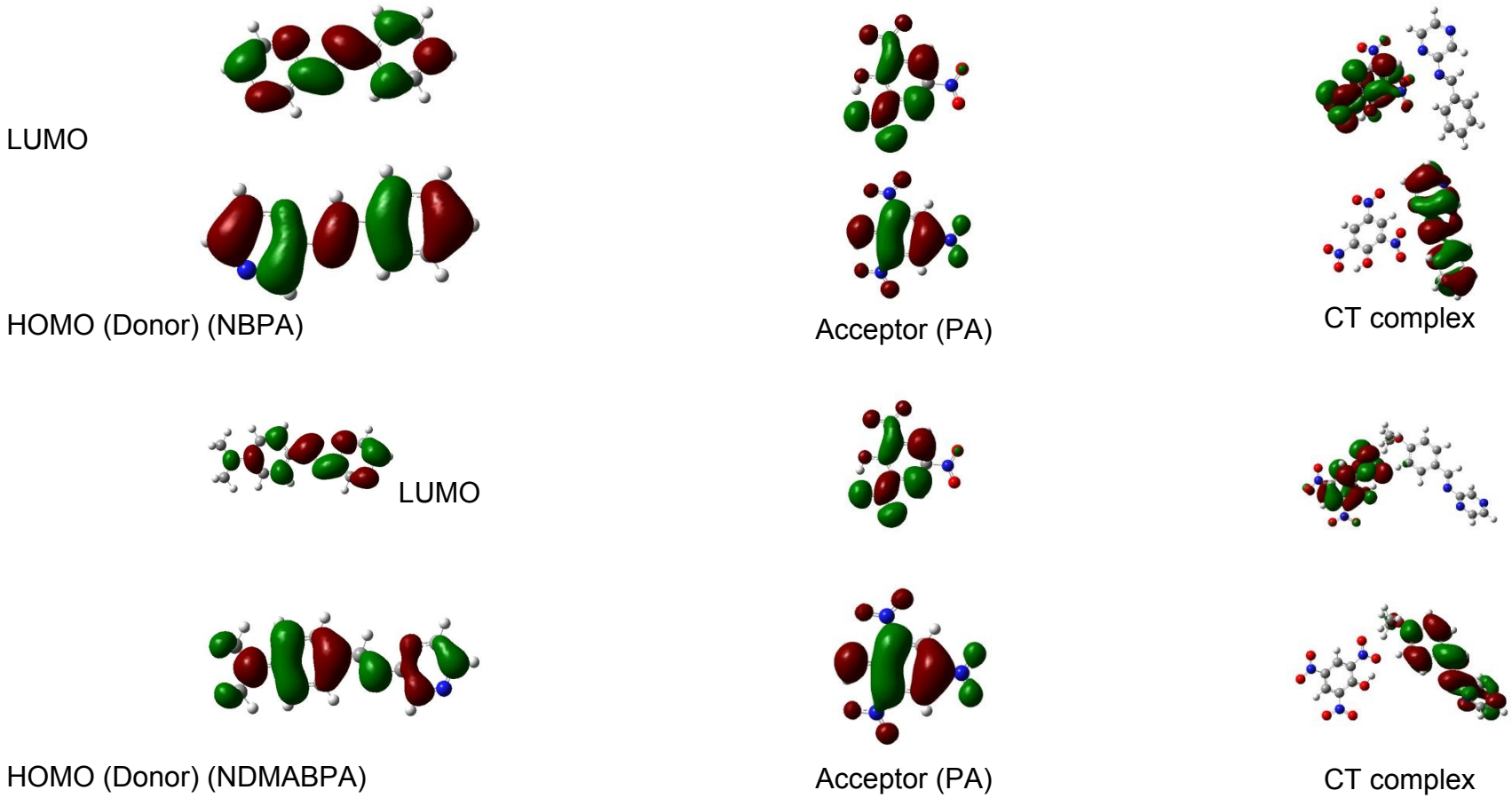

Fig. 7. HOMO and LUMO charge density maps of the studied 2-aminopyrazine Schiff base, p-N(CH_3)$_2$-2-aminopyrazine Schiff base (donors), Picric acid (acceptor) and their charge transfer complex using B3LYP/6-311G**

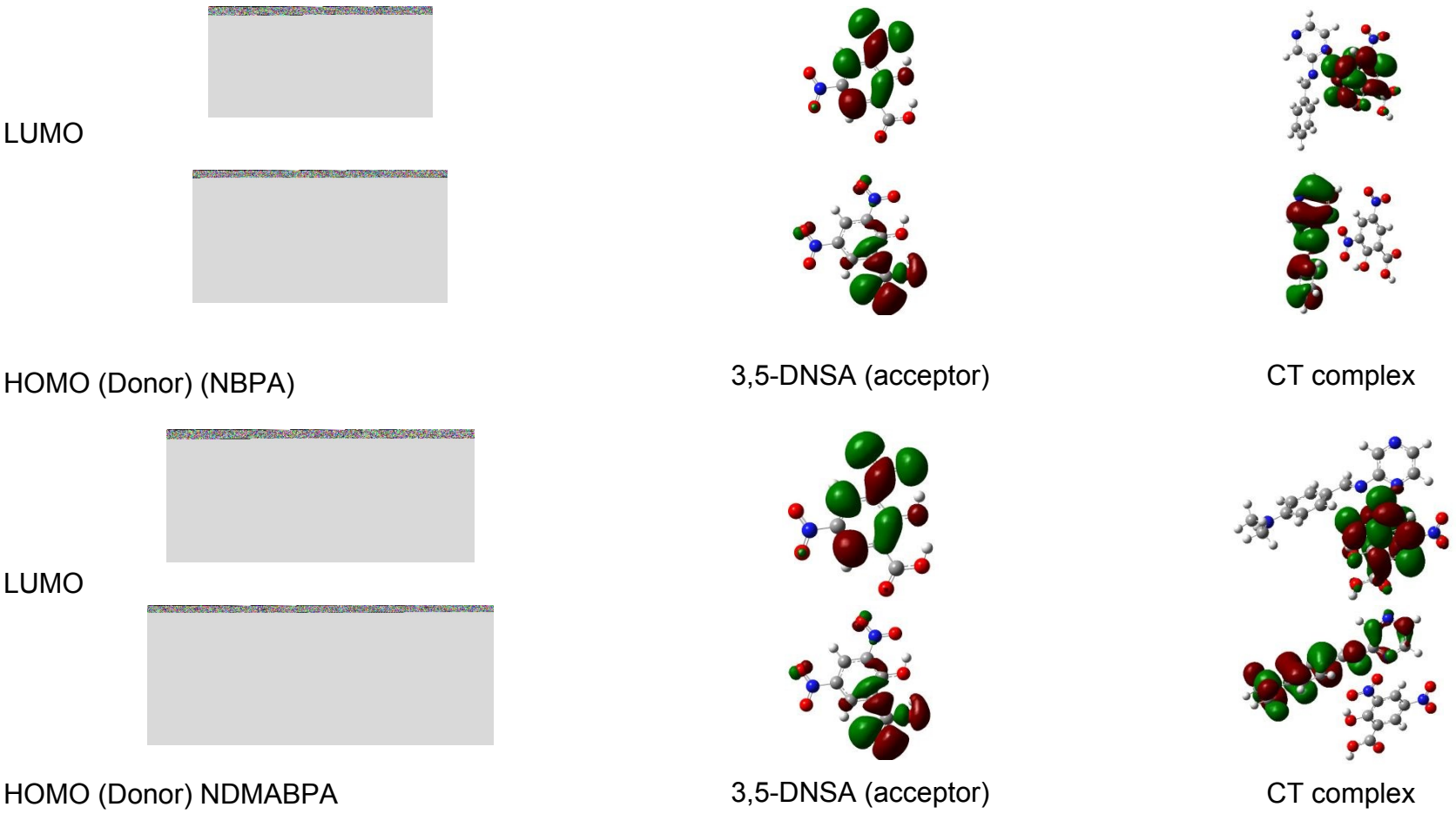

Fig. 8 HOMO and LUMO charge density maps of the studied 2-aminopyrazine Schiff base, p-N$(CH_3)_2$-2-aminopyrazine Schiff base (donors), 3,5-dinitrosalicylic acid (acceptor) and their charge transfer complex using B3LYP/6-311G**

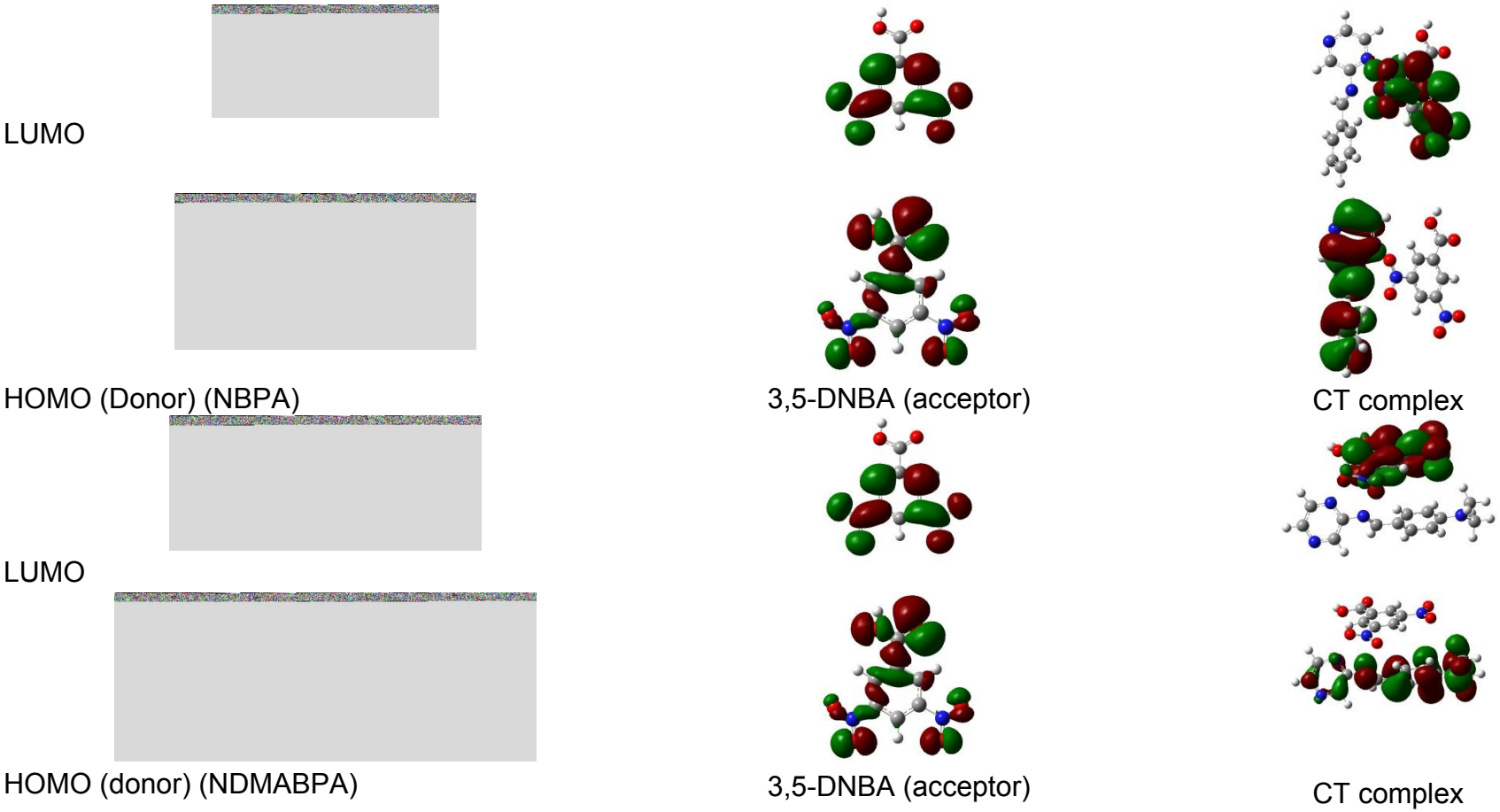

Fig. 9 HOMO and LUMO charge density maps of the studied 2-aminopyrazine Schiff base, p-N$(CH_3)_2$-2-aminopyrazine Schiff base (donors), 3,5-dinitrobenzoic acid (acceptor) and their charge transfer complex using B3LYP/6-311G**

Table 13 NBO charges calculated for the studied 2-aminopyrazine Schiff base donor, Picric, 3,5-dinitrosalicylic and 3,5-dinitrobenzoic acids (acceptors) and their CT complex using B3LYP/6-311G(d,p)

Parameter	Donor	Acceptor	CT complex	Acceptor	CT complex	Acceptor	CT complex
	H	PA		3,5-dNSA		3,5-DNBA	
N1	-0.414		-0.405		-0.407		-0.406
N4	-0.464		-0.469		-0.445		-0.424
N7	-0.504		-0.459		-0.454		-0.455
N11		0.515	0.521				
N12		0.518	0.520				
N13		0.521	0.524				
N15				0.476	0.508		
N16				0.472	0.497		
N14						0.502	0.511
N15						0.502	0.502

comparing to the free donor indicating a CT between the donor and the acceptor via mostly the 2s and 2p orbitals, e.g. the electronic arrangement of donor (N7) is [core]$2s^{1.38}2p^{4.02}3p^{0.01}3d^{0.01}$ while for the CT complex N7 has the electronic arrangement as [core]$2s^{1.35}2p^{4.09}3p^{0.01}3d^{0.01}$. The same trend was found in the case of 3,5-DNSA and 3,5-DNBA. In case of 3,5-DNBA the same results were also obtained, Table 14. The electronic configuration of the N7 is [core]$2s^{1.37}2p^{4.14}3p^{0.01}3d^{0.01}$ and the CT complex was [core]$2s^{1.35}2p^{4.10}3p^{0.01}3d^{0.01}$. In case of p-N-dimethyl-2-aminopyrazine Schiff bases, the same results were obtained as shown in Table S4.

Nonlinear optical properties (NLO)

The distribution of the atomic charges in the complexes is also respected in the determination of the extent and direction of its moment vector which depends on the centers of donor and acceptor charges. The mean polarizability, the anisotropy of the polarizability, the dipole moment, and the first-order hyperpolarizability for the studied free donor (2-aminopyrazine Schiff base) and all CT complexes as well as urea[55] were calculated using the similar level and the found values are tabulated in Table 15. The table also comprises the experimental estimates of urea. The calculated dipole moment value of the free donor (2-aminopyrazine Schiff base) in the gas phase is 2.25 D. The CT complexes have higher dipole moment values than the donor. The polarizabilities and first-order hyperpolarizabilities are described in atomic units (au); the calculated consequences have been adapted into electrostatic units (esu) using adaptation factors of 0.1482×10^{-24} esu for α and 8.6393×10^{-33} esu for β. Urea is a standard pattern used in NLO studies. In this study, urea was selected as a reference as there were no experimental standards of NLO properties of the considered CT complexes. The magnitude of β is one of the main aspects in an NLO system. The calculated values of the polarizability of CT complexes have the range 0.99-5.78 x 10^{-24} (esu). 3,5-DNSA CT complex has the lowest calculated value and 3,5-DNBA CT complex has the highest value. The analysis of β calculated theoretically for the CT complexes shows that 3,5-DNSA CT complex is 11 times higher than urea, while those of the PA and 3,5-DNBA complexes are 6 and 5 higher than the reference material, respectively. Evaluated with urea as a reference

Table 14 Calculated natural charge, natural population and natural electronic configuration of the studied 2-aminopyrazine Schiff base donor, Picric, 3,5-dinitrosalicylic and 3,5-dinitrobenzoic acids (acceptors) and their CT complex using B3LYP/6-311G(d,p)

Complex	Natural charge	Core	Natural population			Natural electronic configuration
			Valence	Rydberg	Total	
Donor (a), (N7)	-0.504	1.9993	5.4860	0.0184	7.5036	[core]$2s^{1.38}2p^{4.02}3p^{0.01}3d^{0.01}$
PA (1), (N13)	0.521	1.9994	4.4286	0.0513	6.4792	[core]$2s^{1.07}2p^{3.36}3s^{0.01}3p^{0.03)}3d^{0.02}$
CT complex (N7)	-0.459	1.9993	5.4414	0.01843	7.4591	[[core]$2s^{1.35}2p^{4.09}3p^{0.01}3d^{0.01}$
(N34)	0.524	1.9994	4.4215	0.0555	6.4763	[core]$2s^{1.06}2p^{3.36}3s^{0.01}3p^{0.03}3d^{0.02}$
3,5-DNSA (2), (N15)	0.476	1.9994	4.4898	0.0350	6.5242	[core]$2s^{1.08}2p^{3.41}3s^{0.01}3p^{0.03}$
CT complex, (N7)	-0.454	1.9993	5.4266	0.0281	7.4540	[core]$2s^{1.36}2p^{4.07}3p^{0.01}3d^{0.01}4p^{0.01}$
(N36)	0.508	1.9995	4.4409	0.0512	6.4917	[core]$2s^{1.10}2p^{3.34}3d^{0.02}4p^{0.03}$
3,5-DNBA (3), (N13)	0.502	1.9996	4.4426	0.0563	6.4985	[core]$2s^{1.10}2p^{3.35}3d^{0.02}4p^{0.03}$
CT complex (N7)	-0.455	1.9993	5.42755	0.0282	7.4550	[core]$2s^{1.35}2p^{4.08}3p^{0.01}3d^{0.01}4p^{0.01}$
(N34)	0.511	1.9996	4.4342	0.0548	6.4885	[core]$2s^{1.09}2p^{3.34}3s^{0.01}3d^{0.02}4p^{0.03}$

Table 15 Calculated total static dipole moment (μ), the mean polarizability <α>, anisotropy of the polarizability Δα and the first-order hyperpolarizability <β > configuration for the studied 2-aminopyrazine Schiff base donor, Picric, 3,5-dinitrosalicylic and 3,5-dinitrobenzoic acids (acceptors) and their CT complex using B3LYP/6-311G(d,p)

Property		Donor	Acceptor	CT complex	Acceptor	CT complex	Acceptor	CT complex
	Urea	H	PA		3,5-dNSA		3,5-DNBA	
μ, D	1.3197	2.2510	1.8975	2.4927	3.9698	5.7528	3.7529	2.7038
αxx, a.u.	-	-65.3884	-106.1316	-167.6139	-105.9304	-174.6036	-108.0481	-142.0198
αyy	-	-80.1202	-108.2568	-169.8679	-118.8258	-169.653	-87.0213	-184.4457
αzz	-	-84.4154	-84.3036	-175.875	-86.5795	-177.2259	-81.495	-176.407
αxy	-	2.4106	3.4958	-8.7959	4.9395	5.0363	-7.5274	16.6365
αxz	-	0	-0.0036	-17.5151	0.0039	15.3821	0	13.3805
αyz	-	0	0.0006	6.5091	-0.0048	-4.3637	0	-12.9778
<α> esu	-	$-1.1358x10^{-23}$	$-1.4755x10^{-23}$	$-2.5360x10^{-23}$	$-1.538x10^{-23}$	$-2.5761x10^{-23}$	$-1.3662x10^{-23}$	$-2.4842x110^{-23}$
Δα, esu	-	$2.5616X10^{-24}$	$3.4033x10^{-24}$	$1.0961x10^{-24}$	$4.1662x10^{-24}$	$0.9871x10^{-24}$	$3.5963x10^{-24}$	$5.7846x10^{-24}$
βxxx	-	-18.1404	-58.2773	80.5438	71.581	-160.1789	-2.765	-12.3569
βxxy	-	1.7806	-0.7731	-40.5254	25.9008	-60.8981	35.5277	26.4797
βxyy	-	26.7198	20.0168	14.1447	-30.791	19.7029	-36.5708	38.4834
βyyy	-	63.9512	-14.9933	-51.334	38.4414	-132.5148	69.4985	31.1595
βxxz	-	0	-0.0089	-8.7656	0.024	15.3176	0	1.9353
βxyz	-	0	-0.0004	-6.364	-0.0007	-12.9682	0	-17.8586
βyyz	-	0	0.0041	13.5826	0.0334	1.1008	0	40.3243
βxzz	-	-8.4632	-1.8796	-13.8722	-0.7307	-13.0815	0.1683	-13.1509
βyzz	-	-7.4781	0.1695	-17.9363	3.2008	-14.5026	-3.0908	-6.1305
βzzz	-	0	-0.0012	2.0971	-0.0087	-7.1282	0	-18.887
<β>, esu	$0.1947x10^{-30}$	$0.5033x10^{-30}$	$0.3720x10^{-30}$	$1.1793x10^{-30}$	$0.6784x10^{-30}$	$2.2345x10^{-30}$	$0.9434x10^{-30}$	$0.5014x10^{-30}$

substance, all the studied CT complexes have higher polarizability and first-order hyperpolarizability values indicating that they are expected to be an applicable candidate for NLO substances. The CT complexes have higher dipole moment values than the donor. The calculated values of the polarizability of CT complexes have the range 4.53-9.74 x 10^{-24} (esu). 3,5-DNSA CT complex has the lowest calculated value and PA CT complex has the highest value. The analysis of β calculated theoretically for the CT complexes shows that PA CT complex is 37 times higher than that of urea, while those of the 3,5-DNSA and 3,5-DNBA complexes are 23 and 6 times higher than the reference material, respectively, Table S5. Compared with urea as a reference substance, all the studied CT complexes have higher polarizability and first-order hyperpolarizability values indicating that they are expected to be also an applicable candidate for NLO substances.

Molecular Electrostatic Potential Surfaces

The MEP determines how attractive or repulsive region of the molecule is to a proton positioned at any point round the molecule.[56] The MEP surfaces were analysed by the DFT method (B3LYP) and basis set (6-311G**) for geometry optimization, as presented in Figs. 10-12. The colour schematic for the MEP surface is as follows, red for electron-rich, partially negative charge; blue for electron-deficient, partial positive charge; light blue for slightly electron-deficient region; yellow for slightly electron-rich region; green for neutral (zero potential).[57] The acceptors (PA, 3,5-DNSA and 3,5-DNBA), MEP plot is distinguished by a positive region (blue), located at the centre. The negative charge region comes from N atoms of CH=N group of the donors. As can be seen from MEP of the investigated CT complexes as shown in Figs. 10-12, the regions having the negative potential are over the electronegative atoms, and regions of negative electrostatic potential are usually connected with the lone pair of electronegative atoms. The highest negative potential is on the CH=N, while the greatest positive regions are over the hydrogen atoms. The carbon atoms appear to have zero potential. The most reactive sites are CH=N group of the donors as clear from MEP and electrostatic potential surfaces as shown in Figs. 10-12. The donors (2-aminopyrazine Schiff base and p-N-dimethyl-2-aminopyrazine Schiff base) major negative region (red) are located on the N atom and the donors interacts with the acceptors (PA, 3,5-DNSA and 3,5-DNBA) positive region. These results verify the electron transfer from n-electrons of the N7 atom of 2-aminopyrazine Schiff base and p-N-dimethyl-2-aminopyrazine Schiff base to NO_2 groups of PA, 3,5-DNSA and 3,5-DNBA acceptors.

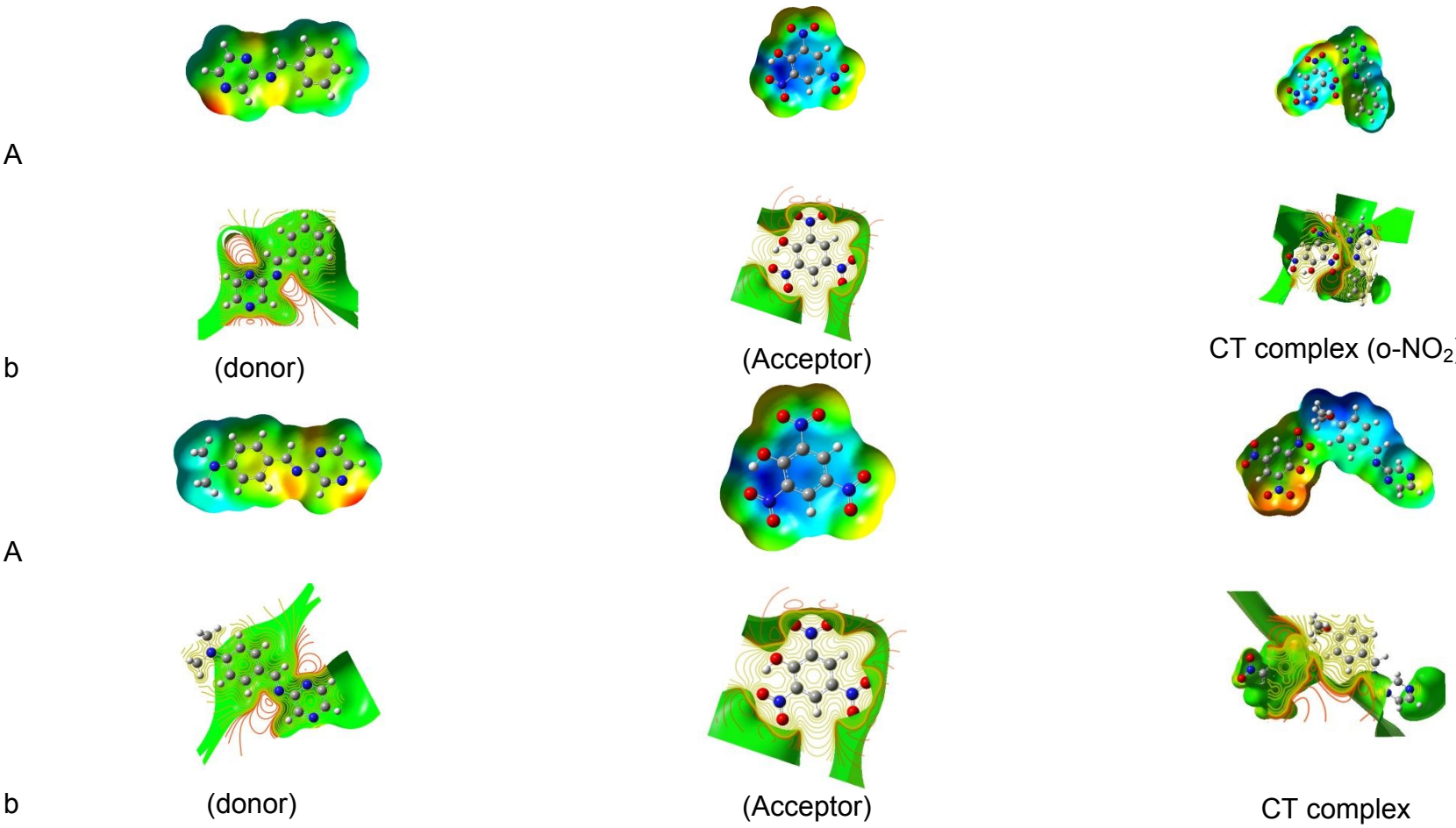

Fig. 10. Molecular electrostatic potential (a) and contours electrostatic potential (b) surfaces of the 2-aminopyrazine Schiff base, p-N-dimethyl-2-aminopyrazine Schiff base (donor), picric acid (acceptor) and their charge transfer complex using B3LYP/6-311G**

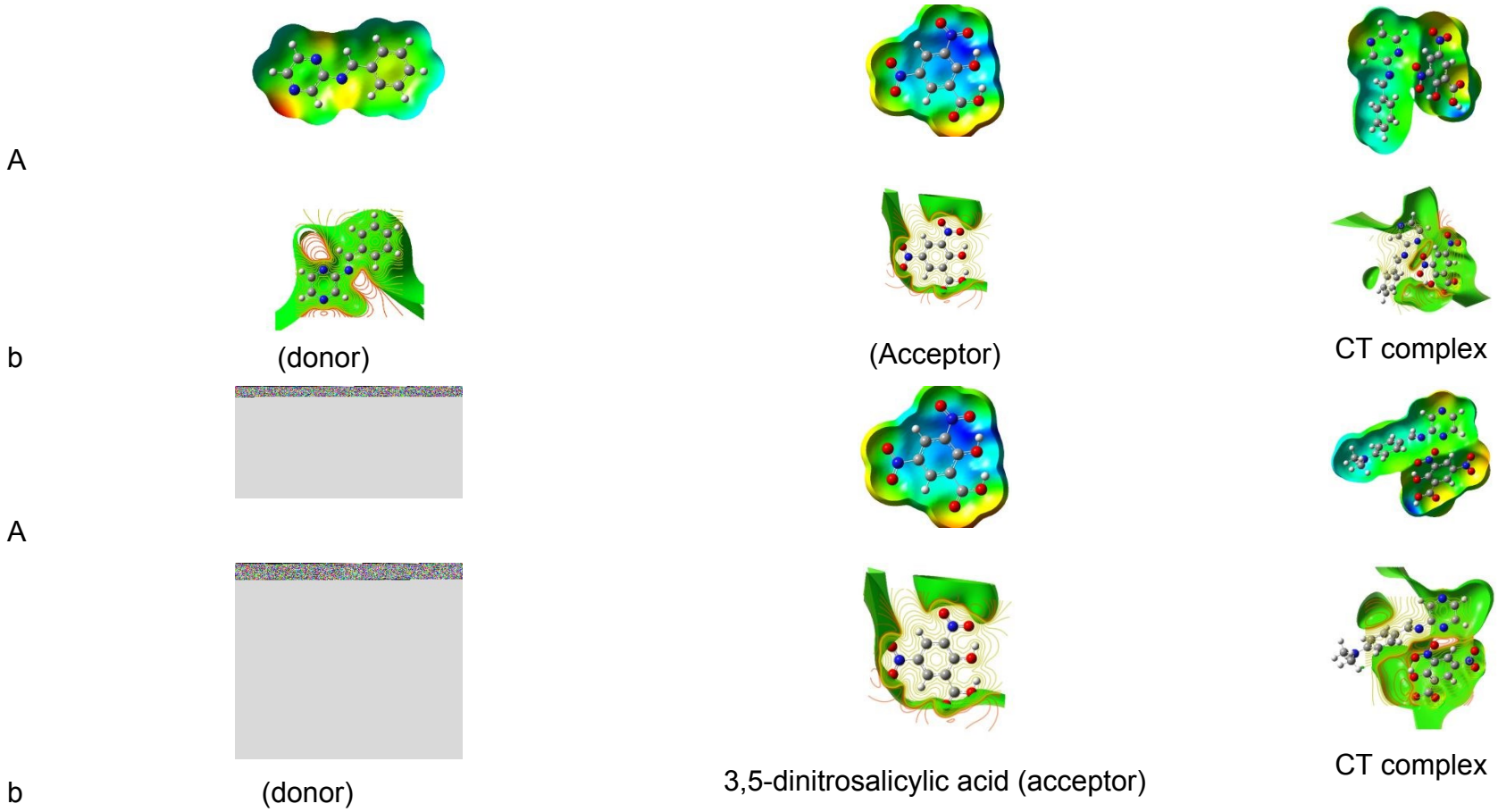

Fig. 11. Molecular electrostatic potential (a) and contours electrostatic potential (b) surfaces of the 2-aminopyrazine Schiff base, p-N-dimethyl-2-aminopyrazine Schiff base (donors), 3,5-dinitrosalicylic acid (acceptor) and their charge transfer complex using B3LYP/6-311G**

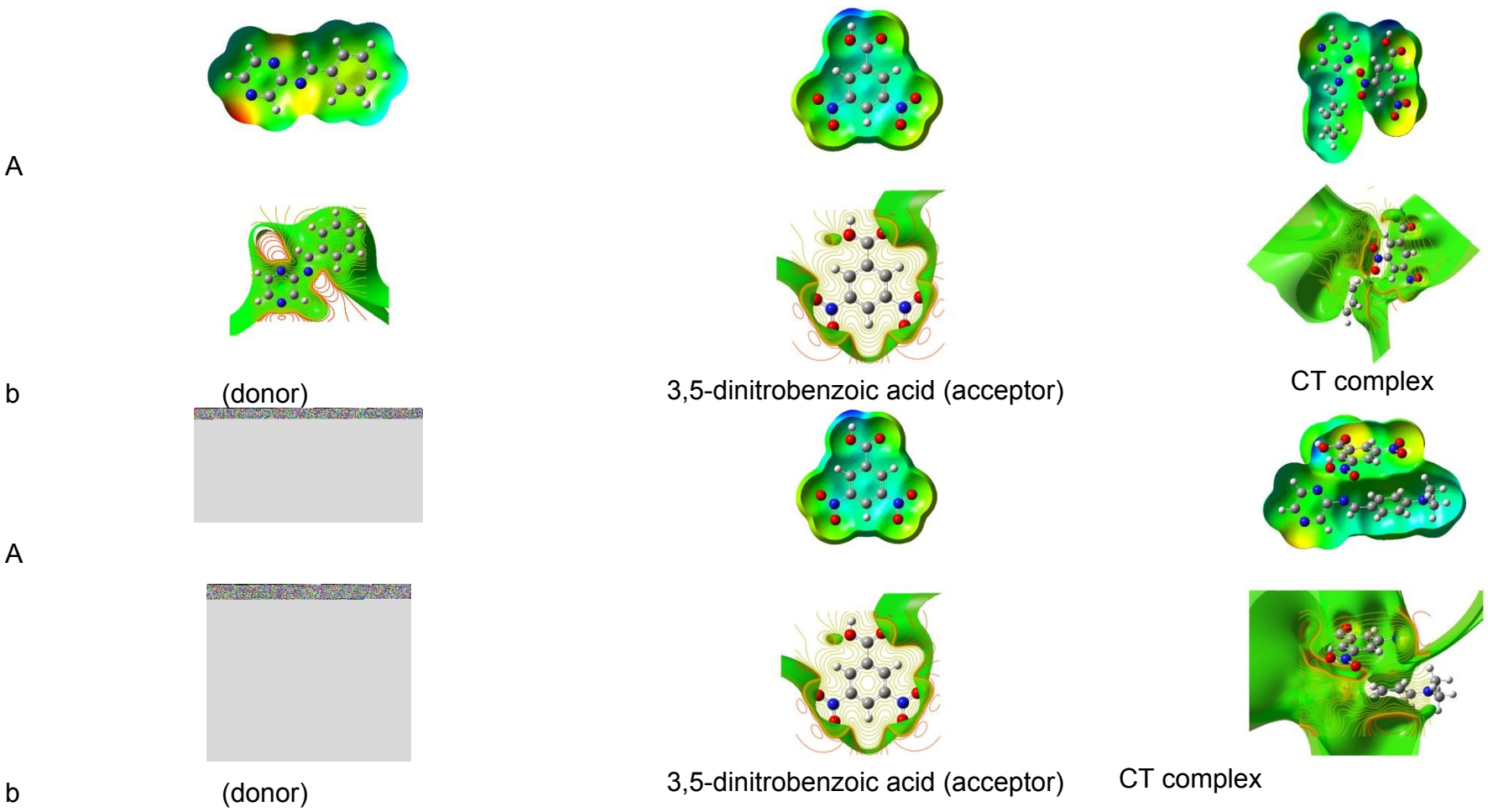

Fig. 12. Molecular electrostatic potential (a) and contours electrostatic potential (b) surfaces of the 2-aminopyrazine Schiff base, p-N-dimethyl-2-aminopyrazine Schiff base (donors), 3,5-dinitrobenzic acid (acceptor) and their charge transfer complex using B3LYP/6-311G**

View Article Online
DOI: 10.1039/D0NJ05397J

TD-DFT studies

TD-DFT calculations were brought out at the same level of theory (B3LYP/6-31G(d,p)) to clarify the origin of electronic spectra, using polarizable continuum solvation method, PCM, PCM-TD-DFT. In PCM the solute part remaining inside cavity, whereas the solvent part (ethanol) denoted as a structureless material. In PCM method, the solvent is also illustrated by its dielectric constant and other macroscopic parameters. TD-DFT calculations of 2-aminopyrazine Schiff base (NBPA) and p-N-dimethyl-2-aminopyrazine Schiff base (NDMABPA) → PA, 3,5-DNSA and 3,5-DNBA were carried out on model representing their molecular structures. If the occupied FMO is donors and the empty FMO is acceptors, the corresponding transition could be CT process. When both the occupied and unoccupied molecular orbitals are local on the same moiety of a given molecule, the transition should be respected as internal transition.[58] The theoretical spectrum of NBPA → PA is characterized by six bands at 396, 357, 355, 336, 334 and 331 nm corresponding to HOMO-1→LUMO, HOMO-1 → LUMO+1, HOMO-2 → LUMO, HOMO-4 → LUMO, HOMO-3 → LUMO and HOMO-1/HOMO → LUMO+3 in that order. The transition at 396 nm corresponds to 48.9% contribution from HOMO-1→LUMO (n-π*) transition, whereas the second excitation band at 357 nm is due to 47.7% contribution, HOMO-1 → LUMO+1, (π-π*) transition, the third excitation band at 355 nm is corresponding to 48.55% contribution, HOMO-2 → LUMO (π-π*) transition, the fourth excitation band at 336 nm is assigned to 79.03% contribution, HOMO-4 → LUMO (π-π*) transition, the fifth excitation band at 334 nm is corresponding to 43.26% contribution, HOMO-3 → LUMO (π-π*) and the sixth excitation band at 331 nm is attributed to 31.16% contribution, HOMO-1/HOMO → LUMO+3 (π-π*) transition. Hence, the vertical excitation energy states are S0 → S2, S0 → S3, S0 → S3, S0 → S4, S0→ S4 and S0→ S5, respectively, are the only allowable transition states with effective oscillator strengths in ethanol. The explanations of FMO's orbitals and transfer of the electron density of NBPA → PA complexes, which are involved in the electronic transitions are given in Fig. 13. While the lowest energy transition at 396 nm is π–π* in nature within PA molecule, the band at 357 nm is allocated for π–π* within NBPA. Six bands are observed in the TD-DFT spectrum (Fig. 14) of NBPA → 3,5-DNSA complexes at 418, 365, 351, 338, 334 and 315 nm due to the following transitions; HOMO-1 → LUMO, HOMO-2 → LUMO, HOMO-3 → LUMO, HOMO-4→ LUMO, HOMO-1→LUMO+2 and HOMO-2 → LUMO+1. The transition at 418 nm is matching to 48.41% contribution from HOMO-1→LUMO (n-π*) transition, while the second excitation band at 365 nm corresponds to 47.49% contribution,

HOMO-2 → LUMO, (π-π*) transition, the third excitation band at 351 nm is related to 44.13% contribution, HOMO-3 → LUMO, (π-π*) transition, the fourth excitation band at 338 nm is corresponding to 43.05% contribution, HOMO-4→ LUMO (π-π*) transition, the fifth excitation band at 334 nm is attributed to 32.40% contribution, HOMO-1→LUMO+2 (π-π*) and the sixth excitation band at 315 nm is corresponding to 48.08% contribution, HOMO-2 → LUMO+1 (π-π*) transition. The vertical excitation energy states are S0 → S2, S0 → S3, S0 → S4, S0 → S5, S0→ S4 and S0→ S4, respectively, are the only permitted transition states with great oscillator strengths in ethanol. The lowermost energy band has a ground state combined of π system of NBPA and excited state contained upon the π* system of 3,5-DNBA molecule forming CT transition (Fig. 15). For NBPA → 3,5-DNBA. Five bands were computed at 383, 359, 332, 323 and 314 nm analogous to HOMO-1 → LUMO/ LUMO+1, HOMO-1 → LUMO/LUMO+1, HOMO-1/HOMO → LUMO+2, HOMO-3 → LUMO/LUMO+1 and HOMO-8 → LUMO/LUMO+1, respectively. The transition at 383 nm is due to 42.11% contribution from HOMO-1 → LUMO/ LUMO+1 (π -π*) transition, while the second excitation band at 359 nm is assigned to 5.28% contribution, HOMO-1 → LUMO/LUMO+1, (π-π*) transition, the third excitation band at 332 nm is matching to 33.28% contribution, HOMO-1/HOMO → LUMO+2, (π-π*) transition, the fourth excitation band at 323 nm is equivalent to 42.32% contribution, HOMO-3 → LUMO/LUMO+1, (π-π*) transition and the fifth excitation band at 314 nm is resultant to 16.02% contribution, HOMO-8 → LUMO/LUMO+1, (π-π*) transition. The vertical excitation energy states are S0 → S2, S0 → S3, S0 → S4, S0 → S5 and S0→ S9, respectively, are the only accepted transition states with intense oscillator strengths in ethanol. Assignment of the conformations of HOMO-1 and LUMO, showed that the lowest energy transition at 383 nm is the picture of CT transition. The explanations of the highest energy transitions are given in Fig. 10. In case of NDMABPA → PA, four bands are detected in the TD-DFT spectrum (Fig. S3) at 1127, 892, 422 and 395 nm due to the successive transitions; HOMO → LUMO, HOMO → LUMO+1, HOMO → LUMO+4, and HOMO-14 → LUMO+1, respectively. The transition at 1127 nm corresponds to 95.67% contribution from HOMO → LUMO CT transition, while the second excitation band at 892 nm refers to 95.07% contribution, HOMO → LUMO+1, CT transition, the third excitation band at 422 nm is agreeing to 99.06% contribution, HOMO → LUMO+4, (π-π*) transition, the fourth excitation band at 395 nm is resembling to 34.04% contribution, HOMO-14 → LUMO+1, (π-π*) transition. The vertical excitation energy states are S0 → S1, S0 → S2, S0 → S4 and S0 → S16, respectively, are the only agreed transition

states with deep oscillator strengths in ethanol. The lowest energy band (1127 nm) has a ground state composed of π system of NDMABPA and excited state contained upon the π* system of PA molecule forming CT transition, (Fig. S3). For NDMABPA → 3,5-DNSA, four bands are found at 440, 390, 370 and 339 nm corresponding to the succeeding transitions; HOMO-1 → LUMO, HOMO-2 → LUMO, HOMO → LUMO+2, and HOMO-4 → LUMO, respectively. The transition at 440 nm corresponds to 49.58% contribution from HOMO-1 → LUMO (π -π*) transition, while the second excitation band at 390 nm is due to 46.95% contribution, HOMO-2 → LUMO, (π-π*) transition, the third excitation band at 370 nm is subsequent to 44.13% contribution, HOMO → LUMO+2, (π-π*) transition, the fourth excitation band at 339 nm is consistent to 43.63% contribution, HOMO-4 → LUMO, (π-π*) transition. The vertical excitation energy states are S0 → S2, S0 → S3, S0 → S3 and S0 → S5, respectively, are the only tolerated transition states with powerful oscillator strengths in ethanol. Assignment of the compositions of HOMO-1 and LUMO, revealed that the lowest energy transition at 440 nm is the picture of CT transition. The narratives of the highest energy transitions are provided in the supporting information (Fig. S4). For NDMABPA → 3,5-DNBA, (Fig. S5), four bands are found at 385, 372, 361 and 336 nm conforming to the successive transitions; HOMO-1 → LUMO, HOMO → LUMO+3, HOMO-2/HOMO-3 → LUMO, and HOMO-3 → LUMO+1, respectively. The transition at 385 nm is conforming to 39.70% contribution from HOMO-1 → LUMO (π -π*) transition, while the second excitation band at 372 nm is agreeing to 43.99% contribution, HOMO → LUMO+3, (π-π*) transition, the third excitation band at 361 nm is assigned to 37.30% contribution, HOMO-2/HOMO-3 → LUMO, (π-π*) transition, the fourth excitation band at 336 nm is equivalent to 46.89% contribution, HOMO-3 → LUMO+1, (π-π*) transition. The vertical excitation energy states are S0 → S2, S0 → S4, S0 → S3 and S0 → S4, respectively, are the only acceptable transition states with brilliant oscillator strengths in ethanol. The lowest energy band at 385 has a ground state composed of π system of NDMABPA → 3,5-DNBA and excited state contained upon the π* system of 3,5-DNBA molecule forming CT transition.

View Article Online
DOI: 10.1039/D0NJ05397J

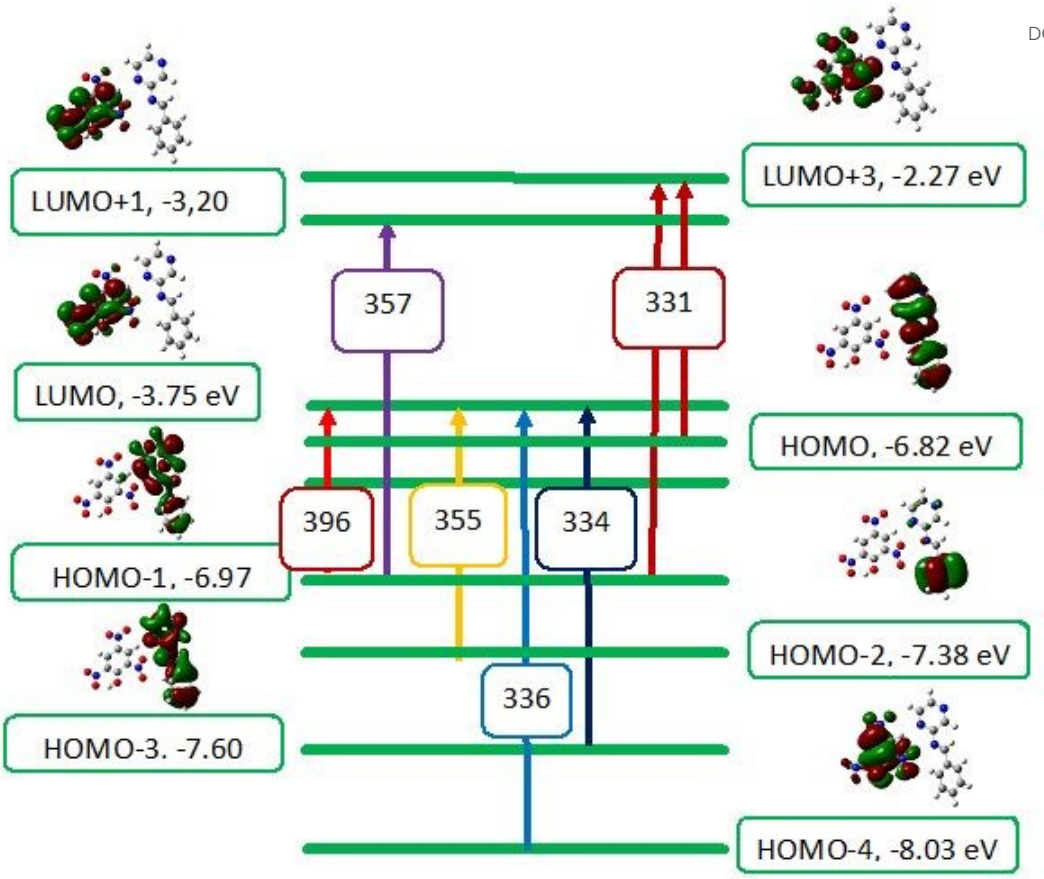

Fig. 13. Frontier molecular orbitals involved in the electronic absorption transitions of NBPA → PA calculated at TD-B3LYP/6-31G(d,p) level of theory.

View Article Online
DOI: 10.1039/D0NJ05397J

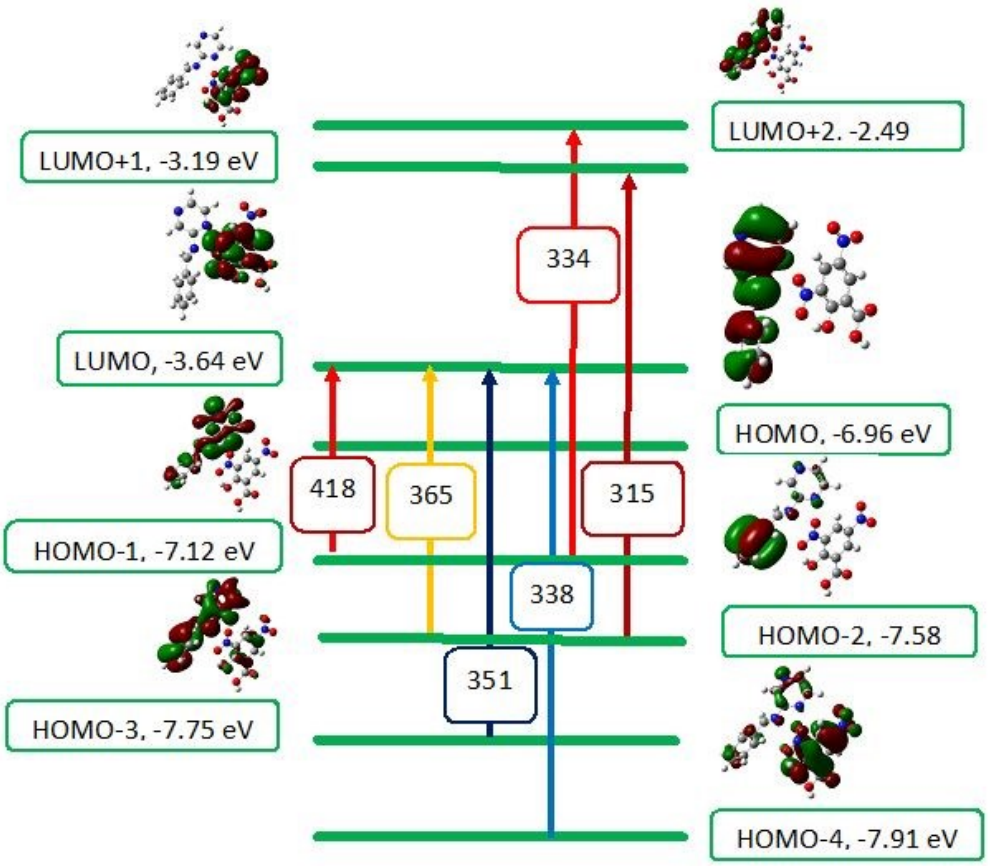

Fig. 14. Frontier molecular orbitals involved in the electronic absorption transitions of NBPA → 3,5-DNSA calculated at TD-B3LYP/6-31G(d,p) level of theory.

View Article Online
DOI: 10.1039/D0NJ05397J

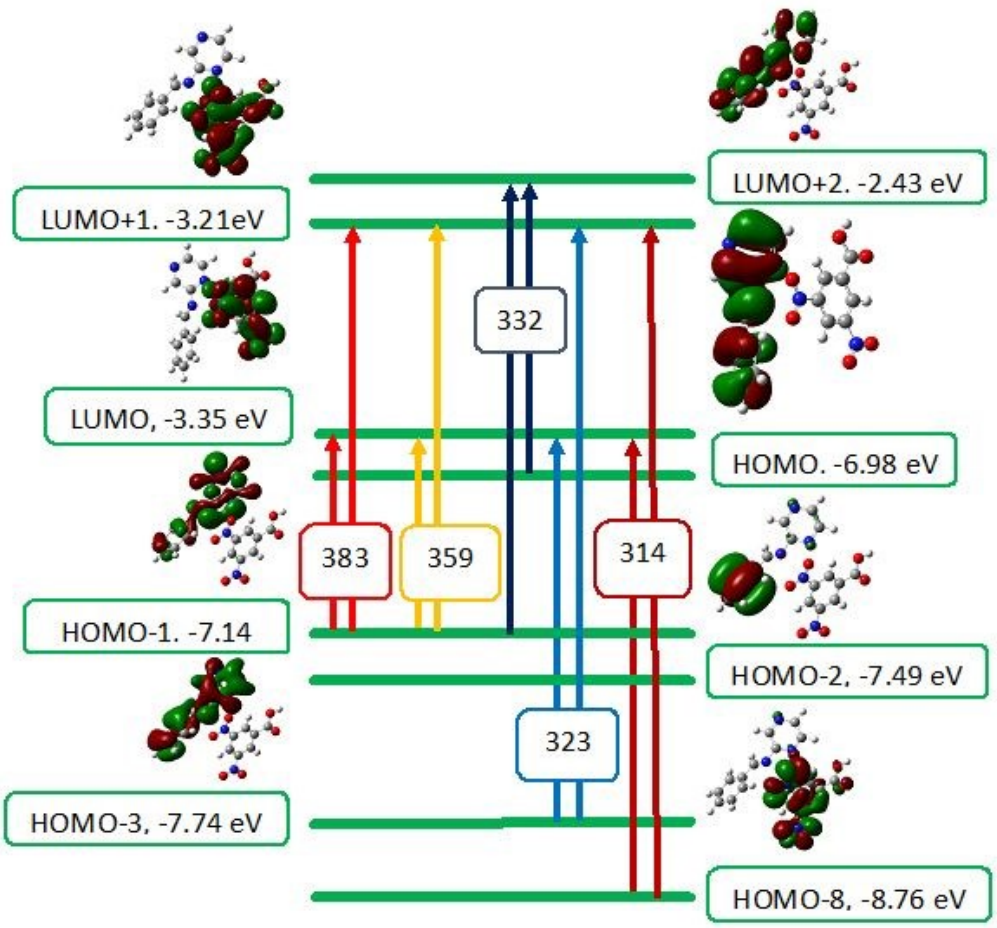

Fig. 15. Frontier molecular orbitals involved in the electronic absorption transitions of NBPA → 3,5-DNBA calculated at TD-B3LYP/6-31G(d,p) level of theory.

Conclusions

New Charge-transfer (CT) solid complexes of pyrazine Schiff bases, derived from 2-aminopyrazine and substituted benzaldehydes (N-benzylidenepyrazin-2-amine, (NBPA) and N-(4-dimethylamino)benzylidene)pyrazin-2-amine) (NDMABPA) with some aromatic nitro compounds have been synthesized and characterized experimentally using ultraviolet-visible (UV-Vis.) absorption spectra, infrared and proton nuclear magnetic resonance (^{1}HNMR) spectroscopy. The respected electronic transition was investigated with the aid of time-dependent density functional calculations. The stoichiometry is 1:1 for the charge transfer interactions between NBPA and NDMABPA as electron donors, and PA, 3,5-DNSA and 3,5-DNBA as π-acceptors in ethanol medium. The physical descriptors like ionization potential of the donors, energy of the CT complexes have been calculated. Furthermore, the PCM-TD-DFT method B3LYP included 6-31G(d,p) and 6-311G(d,p) basis sets were used for

calculations. This study of the CT complexes was achieved by using Gaussian 09 W package with Gauss View 5. This analysis includes bond lengths, bond angles, molecular electrostatic potential maps, description of the important frontier molecular orbital surfaces of the CT complexes and comparison of the natural atomic charge distribution of donors, acceptors and CT complexes. The reactive parameters of acceptors and donors were estimated from the HOMO and LUMO energies. These results also confirm that the PA, 3,5-DNSA and 3,5-DNBA act as the acceptors, while NBPA and NDMABPA are the electron donors.

Conflicts of interest

There are no conflicts to declare.

Acknowledgements

The authors are grateful to the Chemistry Department, Faculty of Science, Cairo University for the calculations.

Notes and References

1. R. D. Kross and V. A. Fassel, *J. Am. Chem. Soc.*, 1957, 79, 38-41.
2. G. Briegleb and H. Della, *Z. Phys. Chem*., 1960, 24, 347-355.
3. R. M. Issa and M. M. Elessawey, *Z. Phys. Chem*., 1973, 253, 96-104.
4. A. M. Hindawey, A. M. G. Nassar, and R. M. Issa, *Acta Chem. Hung*., 1976, 88, 341-349.
5. Y. M. Issa, A. L. El-Ansary, M. Gaber and R. M. Issa, *Acta Chem. Hung*., 1984, 116, 273-281.
6. J. Weinstein and E. McIninch, *J. Am. Chem. Soc.*, 1960, 82, 6064-6067.
7. R. Joshi, A. Kumari, K. Singh, H. Mishra and S. Pokharia, *J. Mol. Struct*., 2020, 1206, 127639.
8. A. M. Hindawey, Y. M. Issa, R. M. Issa, and H. F. Rizk, *Acta Chem. Hung*., 1983, 112, 415-422.
9. M. Gaber, G. B. Mohammed and M. Abdel Ghafer, *J. Chem. Soc. Pak.* 1987, 9, 423-429.
10. O. L. Tombesi, M. A. Frontera, M. A. Tomas and M. A. Bafajoz, *Appl. Spectrosc*., 1993, 47, 123-124.
11. O. L. Tombesi, M. A. Frontera, M. A. Tomas and M. A. Bafajoz, *Appl. Spectrosc.*, 1992, 46, 873-874.
12. Y. M. Issa, N. A. Darwish and H. B. Hassib, *Egypt. J. Chem.*, 1991, 34, 87-93.
13. S. S. Badawy, A. F. Shoukry and Y. M. Issa, *Egypt. J. Chem.*, 1991, 34, 41-49.
14. M. M. Shoukry and R. Kousini, *Bull. Soc. Chem. Fr.*, 1991, 128, 465-468.
15. Z. Afroz, M. Faizan, M. J. Alam, V. H. N. Rodrigues, S. Ahmad and Afaq Ahmad, *J. Mol. Struct.*, 2018, 1171, 438-448.
16. K. M. Al-Ahmary, M. M. Habeeb and S. H. Aljahdali, *J. Mol. Struct.*, 1181, 2019, 48-60.
17. K. M. Al-Ahmary, M. M. Habeeb and S. H. Aljahdali, *J. Mol. Liq.,* 277, 2019, 453–470.
18. S. Soltani, P. Magri, M. Rogalski and M. Kadri, *J. Mol. Struct*., 1175, 2019), 105-116.
19. N. Venkatesh, B. Naveen, A. Venugopal, G. Suresh, V. Mahipal, P. Manojkumar and T. Parthasarathy, *J. Mol. Struct*., 1196, 2019, 462-477.
20. A. El-Dissouky, T. E. Khalil, H. A. Elbadawy, D. S. El-Sayed, A. A. Attia and S. Foro, *J. Mol. Struct.*, 1200, 2020, 127066.
21. I. M. Khan, M. Islam, S. Shakya, K. Alam, N. Alam and M. Shahid, *Bioorg. Chem*. 99, 2020, 103779.

22. A. Karmakar, P. Bandyopadhyay, S. Banerjee, N. C. Mandal and B. Singh, *J. Mol. Liq.*, 299, 2020, 112217.
23. A. Thamarai, R. Vadamalar, M. Raja, S. Muthuc, B. Narayana, P. Ramesh, R. R. Muhamed, S. Sevvanthi and S. Aayisha, *Spectrochim. Acta, Part A*, 226, 2020, 117609.
24. V. Abbu, V. Nampally, N. Baindla and P. Tigulla, *J. Solution Chem*., 2019, 48, 61-81.
25. A. I. Vogel, *Practical Organic Chemistry Including Quantitative Organic Analysis*, 5th ed., Longmans, London, UK, 1991.
26. A. L. El Ansary, N. A. Darwish, Y. M. Issa and H. B. Hassib, *Egypt. J. Chem*., 1990, 33, 129-145.
27. A. M. Hindawey, Y. M. Issa, Y. A. Marghalani and R. M. Issa, *Monsatsh. Chem*., 1980, 111, 1143-1150.
28. M.J. Frisch, G.W. Trucks, H.B. Schlegel, G.E. Scuseria, M.A. Robb, J.R. Cheeseman, G. Scalmani, V. Barone, B. Mennucci, G.A. Petersson, H. Nakatsuji, M. Caricato, X. Li, H.P. Hratchian, A.F. Izmaylov, J. Bloino, G. Zheng, J.L. Sonnenberg, M. Hada, M. Ehara, K. Toyota, R. Fukuda, J. Hasegawa, M. Ishida, T. Nakajima, Y. Honda, O. Kitao, H. Nakai, T. Vreven, J.A. Montgomery Jr., J.E. Peralta, F. Ogliaro, M. Bearpark, J.J. Heyd, E. Brothers, K.N. Kudin, V.N. Staroverov, R. Kobayashi, J. Normand, K. Raghavachari, A. Rendell, J.C. Burant, S.S. Iyengar, J. Tomasi, M. Cossi, N. Rega, J.M. Millam, M. Klene, J.E. Knox, J.B. Cross, V. Bakken, C. Adamo, J. Jaramillo, R. Gomperts, R.E. Stratmann, O. Yazyev, A.J. Austin, R. Cammi, C. Pomelli, J.W. Ochterski, R.L. Martin, K. Morokuma, V.G. Zakrzewski, G.A. Voth, P. Salvador, J.J. Dannenberg, S. Dapprich, A.D. Daniels, O. Farkas, J.B. Foresman, J.V. Ortiz, J. Cioslowski and D.J. Fox, *Gaussian 09, Revision A1*, Gaussian Inc., Wallingford, CT. 2009.
29. A. D. Becke, *J. Chem. Phys*., 1993, 98, 5648-5652.
30. C. Lee, W. Yang and R. G. Parr, *Phys. Rev. B: Condens. Matter Mater. Phys.*, 1988, 37, 785-789.
31. M. J. Frisch, J. A. Pople and J. S. Binkley, *J. Chem. Phys.*, 1984, 80, 3265-3269.
32. T. Schaefer, S. R. Salman and T. A. Wildman, *J. Am. Chem. Soc*., 1980,102, 107-110.
33. P. J. Hay and W. R. Wadt, *J. Chem. Phys*., 1985, 82, 270-283.
34. R. Dennington, T. Keith, J. Millam and K. S. Shawnee Mission, *Gauss View, Version 5*, Semichem. Inc., 2009.

35. N. A. El Ghamaz, M. A. Diab, A. A. El Bindary, A. Z. El Sonbati and H. A. Seyam, *Mater. Sci. Semicond. Process*., 2014, 27, 521-531.
36. A. Z. El-Sonbati, M. A. Diab, A. A. El Bindary and S. M. Morgan, *Spectrochim. Acta, Part A*, 2014, 127, 310-328.
37. J. Chocholoušová, V. Špirko and P. Hobza, *Phys, Chem. Chem. Phys.*, 2004, 6, 37-41.
38. D. Avci, *Spectrochim. Acta, Part A*, 2011, 82, 37-43.
39. D. Avci, A. Başoğlu and Y. Atalay, *Struct. Chem*., 2010, 21, 213-219.
40. D. Avci, H. Cömert and Y. Atalay, *J. Mol. Mod*., 2008, 14, 161-169.
41. L. J. Bellamy, *The Infrared Spectra of Complexes Molecules*, Vol. 1, Chapman & Hall, New York, 1975.
42. L. N. Short and H. W. Thompson, *J. Chem. Soc.*, 1952, 168-187.
43. H. A. Sahyon, A. A. El-Bindary, A. F. Shoair and A. A. Abdellatif, *J. Mol. Liq.*, 2018, 255, 122-134.
44. A. A. El-Bindary, S. M. El-Marsafy and A. A. El-Maddah, *J. Mol. Struct*., 2019, 1191, 76-84.
45. A. A. El-Bindary, E. A. Toson, K. R. Shoueir, H.A. Aljohani and M. M. Abo-Ser, *Appl. Organometal. Chem*., 2020, 34, e5905.
46. C. H. Warren, G. Wettermark and K. Weiss, *J. Am. Chem. Soc.*, 1971, 93, 4658-4663.
47. Y. M. Issa, A. E. El-Kholy and A. L. El-Ansary, *Acta Chim. Hung.*, 1985, 118, 43-48.
48. E. Bosch, C. Ráfols and M. Roses, *Anal. Chim. Acta*, 1995, 302, 109-l 19.
49. D. C. Wheat, *Handbook of Chemistry and Physics*, 50th ed., The Chemical Rubber Company, Ohio, USA, 1970.
50. G. Briegleb, and J. Czekalla and A. Hauser, *Z. Phys. Chem.*, 1959, 21, 99-113.
51. E. Bosch, C. Ráfols and M. Roses, *Anal. Chim. Acta*, 1995, 302, 109-l 19.
52. S. Abdul Rahim, S. Hussain and M. Farooqui, *J. Ultra Chem*., 2016, 12, 71-74.
53. G. Briegleb, *Angew. Chem.*, 1964, 76, 326-341.
54. M. M. Habeeb, A. S. Al-Attas and D. S. Al-Raimi, *Spectrochim. Acta, Part A*, 2015, 142, 196-203.
55. Y. Y. Lin, N. P. Rajesh, P. S. Raghavan, P. Ramasamy and Y. C. Huang, *Mater. Lett*., 2002, 56, 1074-1077.
56. K. M. Al-Ahmary, R. A. Mekheimer, M. S. Al-Enezi, N. M. M. Hamada and M. M. Habeeb, *J. Mol. Liq*., 2018, 249, 501-510.
57. P. Politzer and J. S. Murray, *Theor. Chem. Acc*., 2002, 108, 134-142.

58. O. R. Shehab and A. M. Mansour, *J. Mol. Struct*., 2015, 1093, 186-194.

View Article Online
DOI: 10.1039/D0NJ05397J

Graphical Abstract

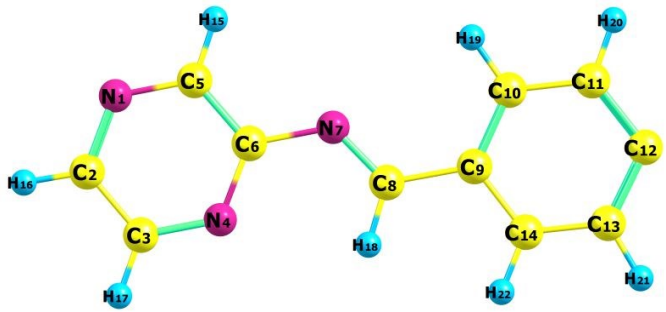

Donor (NBPA)

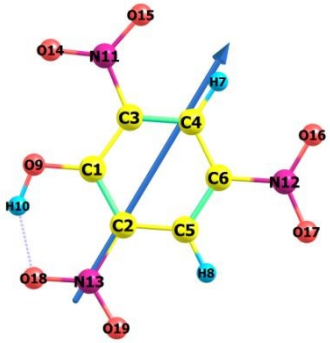

Acceptor (PA)

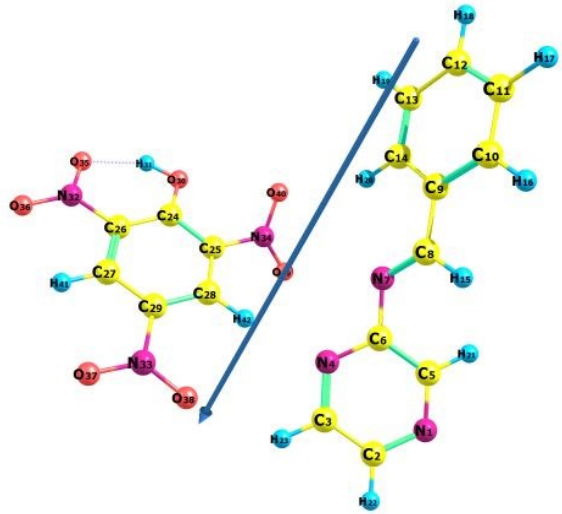

CT complex

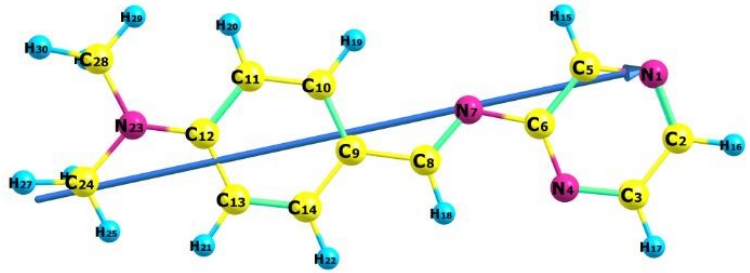

Donor (NDMABPA)

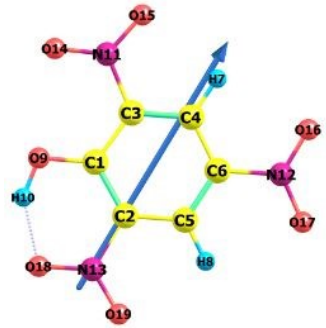

Acceptor (PA)

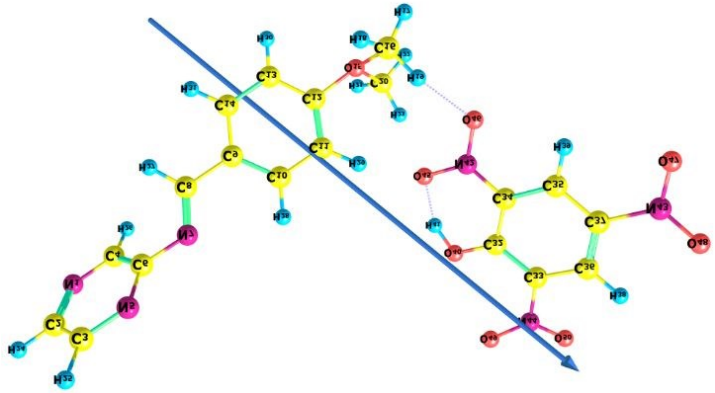

CT complex